

ON THE APPLICATION OF ELLIPTIC FUNCTIONS TO  
STANDARD COSMOLOGY

by

**Hunter Lowe**

B.Sc., University of Northern British Columbia, 2019

THESIS SUBMITTED IN PARTIAL FULFILLMENT OF  
THE REQUIREMENTS FOR THE DEGREE OF  
MASTER OF SCIENCE  
IN  
PHYSICS

UNIVERSITY OF NORTHERN BRITISH COLUMBIA

APRIL 2023

© Hunter Lowe, 2023

**UNIVERSITY OF NORTHERN BRITISH COLUMBIA PARTIAL  
COPYRIGHT LICENCE**

I hereby grant the University of Northern British Columbia Library the right to lend my project/thesis/dissertation to users of the library or to other libraries. Furthermore, I grant the University of Northern British Columbia Library the right to make single copies only of my project/thesis/dissertation for users of the library or in response to a request from other libraries, on their behalf or for one of their users. Permission for extensive copying of this project/thesis/dissertation for scholarly purposes may be granted by me or by a member of the university designated by me. It is understood that copying or publication of this thesis/dissertation for financial gain shall not be allowed without my written permission.

Title of Project/Thesis/Dissertation: \_\_\_\_\_  
\_\_\_\_\_ On the Application of Elliptic Functions to Standard Cosmology \_\_\_\_\_  
\_\_\_\_\_

Author \_\_\_\_\_ Hunter Lowe \_\_\_\_\_ April 2023 \_\_\_\_\_  
Printed Name Signature Date

## Abstract

This thesis provides generalization to known solutions for the scale factor and cosmic time of Friedmann–Lemaître–Robertson–Walker model universes in terms of elliptic functions. In particular the integration of known expressions for the scale factor is used to find new expressions for cosmic time. Various techniques using both the Weierstrass and Jacobi functions are discussed. Plots of physically significant quantities such as redshift and redshift drift are given. Limiting cases provide context for how various cosmic fluids change the dynamics of the universe on the largest scales.

## TABLE OF CONTENTS

<b>Abstract</b>	<b>3</b>
<b>Table of Contents</b>	<b>4</b>
<b>List of Tables</b>	<b>6</b>
<b>List of Figures</b>	<b>7</b>
<b>1 Introduction</b>	<b>8</b>
1.1 Object . . . . .	8
1.2 Related Work . . . . .	8
1.3 Overview . . . . .	9
<b>2 Background: Elliptic Functions and Integrals</b>	<b>11</b>
2.1 Elliptic Integrals . . . . .	11
2.2 Jacobi Elliptic Functions . . . . .	12
2.3 The Weierstrass Elliptic Function . . . . .	18
2.4 The Elliptic Functions . . . . .	20
<b>3 Background: Cosmology</b>	<b>24</b>
3.1 The FLRW Spacetime . . . . .	24
3.2 Distance and Time . . . . .	26
3.3 Cosmic Dynamics . . . . .	28
3.4 General Solution for FLRW Scale Factor . . . . .	32
<b>4 Results</b>	<b>34</b>
4.1 Model Solutions . . . . .	34
4.2 The Spatially-Flat $\Lambda$ CDM Model . . . . .	35
4.3 The Hyperelliptic Integral Method . . . . .	38
4.4 Generalised Model Solution . . . . .	43
4.5 Redshift Drift . . . . .	49
4.6 Limiting Cases . . . . .	56
4.6.1 Dark Energy and Matter . . . . .	57
4.6.2 Dark Energy, Matter, and Spatial Curvature . . . . .	57
4.6.3 Matter, Spatial Curvature, and Radiation . . . . .	58

<b>5</b>	<b>Conclusion</b>	<b>63</b>
<b>A</b>	<b>Numerical Methods</b>	<b>66</b>
A.1	Friedmann Equation Discretization . . . . .	66
<b>B</b>	<b>Calculation of Elliptic Functions and Integrals</b>	<b>70</b>
B.1	Maple . . . . .	70
	<b>Bibliography</b>	<b>71</b>

**LIST OF TABLES**

2.1 The Jacobi elliptic functions and their quotients. . . . . 13

## LIST OF FIGURES

2.1	The Jacobi Ellipse with $a = 1$ . The point $P = (x, y)$ on the ellipse projects onto the unit circle to point $Q = (cn, sn)$ . . . . .	14
2.2	The fundamental period parallelogram for the case of $\Delta > 0$ . . . . .	21
2.3	The fundamental period parallelogram for the case of $\Delta < 0$ . . . . .	21
4.1	Three methods for plotting the Planck universe. Equation (4.12) is the <i>Lemaître solution</i> , equation (4.8) is the <i>standard solution</i> , and finally a <i>numerical solution</i> curve is shown as a sanity check. . . . .	37
4.2	The hyperelliptic solution <i>Jacobi</i> versus the Lemaître solution <i>Weierstrass</i> . . . . .	43
4.3	Numerical data versus analytical data for the full Planck universe. . .	46
4.4	Numerical data versus analytical data for a collapsing universe with matter, dark energy, curvature, and radiation. . . . .	48
4.5	Comparison of exact redshift drift and a realistic approximation. . . .	52
4.6	The order of magnitude for the change in redshift drifts over 100 years. . .	53
4.7	Redshift drift versus redshift for an object in our universe. Redshift drift is increasing with cosmic time for all times, but redshift may be increasing or decreasing with cosmic time for some times. . . . .	54
4.8	Redshift versus cosmic time of an object in our universe. . . . .	55
4.9	Redshift drift versus cosmic time of an object in our universe. . . . .	55
4.10	The “stalling” or “loitering” effect of dark energy highlighted with a cyclic universe. . . . .	60
4.11	The “looping” effect of radiation compared to matter only. . . . .	61
A.1	The agreement between exact and numerical results for cosmic scale. . . .	68
A.2	The agreement between exact and numerical results for cosmic time. . . .	68

# Chapter 1

## Introduction

### 1.1 Object

The objective of this thesis is to provide new special function solutions to problems in cosmology. It is desired to do so in such a way as to display intuitively useful insight into obtaining and interpreting these solutions. The use of Jacobi and Weierstrass elliptic functions for modelling Friedmann–Lemaître–Robertson–Walker (FLRW) universes is a core component of this work. Modern computing tools will be used to explore the results obtained throughout this thesis.

### 1.2 Related Work

Elliptic integrals and functions have been used in many areas of physics for over one hundred years. A classic example is the full solution to the simple pendulum where one does not make the small angle approximation [11]. These special integrals and functions arise naturally in a wide variety of physical systems.

General relativity presents many problems that can be analysed using various special functions. The Schwarzschild geometry, Kerr geometry, and many other spacetimes can be handled in this fashion. Chandrasekhar [4] classifies and details many

orbits in the Schwarzschild geometry in part by using the Jacobi elliptic functions and integrals. This work is further generalised by Scharf [29] and Rodríguez [27]. Many spacetime geometries evidently provide a framework where physical phenomena are readily described using elliptic integrals and functions.

The FLRW spacetime is another environment where special functions may be applied. Edwards [10], D’Ambroise [8], and Steiner [31] each solve for the scale factor of general FLRW universes in terms of special functions. The general solution for the scale factor as a function of conformal time is written in terms of the Weierstrass elliptic function. This type of analysis dates as far back as the founding work done by the titan Lemaître [21, 22]. Elliptic integral techniques are applied by Kharbediya [20] for several types of universes. Edwards and D’Ambroise also look at special cases of the scale factor in terms of the Jacobi elliptic functions. Steiner discusses his results in the context of modelling the time dependence of the energy density of the universe. Aurich and Steiner [32] apply this approach to an investigation into hyperbolic finite volume universes. An explicit formula for luminosity distance as a function of redshift is given by Dabrowski [6]. D’Ambroise [9] provides a resource for solving some nonlinear differential equations in cosmology using special functions.

There are other important model properties for FLRW universes that have not been modelled using special function techniques. Redshift and redshift drift are two important quantities plotted by Liske [13] and Lineweaver [23]. Lobo et al. [15] investigates some higher order changes in redshift drift using an asymptotic series type approach. Understanding the dynamical properties of universe expansion is important for constructing a clearer picture of our cosmos.

### **1.3 Overview**

This thesis is broken down in the following manner. Chapter 2 will provide the necessary background for special functions and integrals used throughout this thesis.

The elliptic integrals are defined in standard fashion, and used to derive the elliptic functions of Jacobi. Trigonometric analogies for these functions help motivate why they might be especially useful to physicists. The elliptic functions of Weierstrass are introduced and related to the elliptic functions of Jacobi. Other functions of Weierstrass are discussed in the context of doing calculus with his elliptic function. General motivation and theory for all elliptic functions is briefly mentioned.

Chapter 3 will contain the core principles of standard cosmology and cosmic dynamics. The FLRW spacetime and how it arises in the framework of general relativity begins the chapter. The concept of measuring space and time in cosmology is introduced. How the distribution of matter and energy changes the scale factor of spacetime is of particular significance. The Friedmann equation and its solution are discussed in detail for the purpose of modelling the scale factor. Chapter 4 will show how known special function solutions for the scale factor can be used to derive new expressions. Attempting to derive new expressions using both the functions of Jacobi and Weierstrass is presented. The results are tested with independent numerical modelling, and subsequently plotted. State of the art data is used to create a benchmark for these results. Redshift and redshift drift are calculated in a new fashion. Limiting cases are broken down to explore the parameter space of the provided solutions. Chapter 5 will conclude this thesis and summarize the results obtained.

# Chapter 2

## Background: Elliptic Functions and Integrals

### 2.1 Elliptic Integrals

Elliptic integrals come in three different basic forms which each involve the integration of radical functions. The integral

$$\begin{aligned} u &= \int_0^y \frac{dy'}{\sqrt{(1-y'^2)(1-k^2y'^2)}} \\ &= \int_0^\phi \frac{d\phi'}{\sqrt{(1-k^2\sin^2\phi')}} \\ &\stackrel{\text{def}}{=} F(y, k) \end{aligned} \tag{2.1}$$

is called the incomplete elliptic integral of the first kind. The integral

$$\begin{aligned} u &= \int_0^y \sqrt{\frac{1-k^2y'^2}{1-y'^2}} dy' \\ &= \int_0^\phi \sqrt{1-k^2\sin^2\phi'} d\phi' \\ &\stackrel{\text{def}}{=} E(y, k) \end{aligned} \tag{2.2}$$

is called the incomplete elliptic integral of the second kind. The integral

$$\begin{aligned}
 u &= \int_0^y \frac{dy'}{(1 - \alpha^2 y'^2) \sqrt{(1 - y'^2)(1 - k^2 y'^2)}} \\
 &= \int_0^\phi \frac{d\phi'}{(1 - \alpha^2 \sin^2 \phi') \sqrt{(1 - k^2 \sin^2 \phi')}} \\
 &\stackrel{\text{def}}{=} \Pi(y, \alpha^2, k)
 \end{aligned} \tag{2.3}$$

is called the incomplete elliptic integral of the third kind. The preceding integral definitions are provided by Byrd and Friedman [2]. The substitution  $y = \sin \phi$  is a useful change of variables.

The **elliptic modulus**  $k$  is a complex number in general, but often  $k$  is limited to the range of values  $0 < k < 1$ . Some sources prefer to use the **elliptic parameter**  $m$  which is related to the elliptic modulus by  $m = k^2$ . The **complimentary elliptic modulus**  $k'$  often is used, and is related to the elliptic modulus by  $k' = \sqrt{1 - k^2}$ . The **elliptic characteristic**  $\alpha^2$  is a complex number in general, but  $\alpha^2$  often is limited to real numbers. The **elliptic argument**  $y$  or  $\phi$  also can take on any complex value, but it's most common to use the ranges  $0 < y \leq 1$  and  $0 < \phi \leq \pi/2$ . When  $y = 1$  the elliptic integrals are said to be **complete**. Note that the change of variables  $y = \sin \phi$  implicitly includes the choice of branch cut  $\sqrt{(1 - t^2)(1 - k^2 t^2)} = \sqrt{(1 - t^2)} \sqrt{(1 - k^2 t^2)}$  in equations (2.1) to (2.3). For the purposes of the results obtained in this thesis, it will be more appropriate to not use this change of variables, though it is still useful to help motivate the elliptic functions of Jacobi, as will be seen in the next section.

## 2.2 Jacobi Elliptic Functions

It is of interest to invert the elliptic integral of the first kind in order to define the Jacobian elliptic functions. The **amplitude** function is defined by  $\phi = \text{am}(u, k)$ . The **sine amplitude** and **cosine amplitude** are defined by  $\sin \phi = \text{sn}(u, k)$  and

$\cos \phi = \text{cn}(u, k)$  respectively. The **delta amplitude** is defined by  $\Delta\phi = \text{dn}(u, k) = \sqrt{1 - k^2 \sin^2 \phi}$ . These functions have properties very similar to the trigonometric functions. Often authors will suppress the modulus and even the argument of an elliptic function to neaten their work.

Table 2.1: The Jacobi elliptic functions and their quotients.

$$\begin{array}{lll}
 \text{ns } u \stackrel{\text{def}}{=} \frac{1}{\text{sn } u} & \text{tn } u \stackrel{\text{def}}{=} \text{sc } u \stackrel{\text{def}}{=} \frac{\text{sn } u}{\text{cn } u} & \text{sd } u \stackrel{\text{def}}{=} \frac{\text{sn } u}{\text{dn } u} \\
 \text{nc } u \stackrel{\text{def}}{=} \frac{1}{\text{cn } u} & \frac{1}{\text{tn } u} \stackrel{\text{def}}{=} \text{cs } u \stackrel{\text{def}}{=} \frac{\text{cn } u}{\text{sn } u} & \text{cd } u \stackrel{\text{def}}{=} \frac{\text{cn } u}{\text{dn } u} \\
 \text{nd } u \stackrel{\text{def}}{=} \frac{1}{\text{dn } u} & \text{ds } u \stackrel{\text{def}}{=} \frac{\text{dn } u}{\text{sn } u} & \text{dc } u \stackrel{\text{def}}{=} \frac{\text{dn } u}{\text{cn } u}
 \end{array}$$

Standard trigonometric functions can be defined by use of the unit circle, and the Jacobi elliptic functions are no different. The sine amplitude and cosine amplitude are projections from a point on an ellipse to the corresponding point on the unit circle. This idea is shown in figure 2.1. Essentially the angle  $\theta$  determines where a point on the ellipse is, and the modulus  $k$  determines how elliptic the shape is.

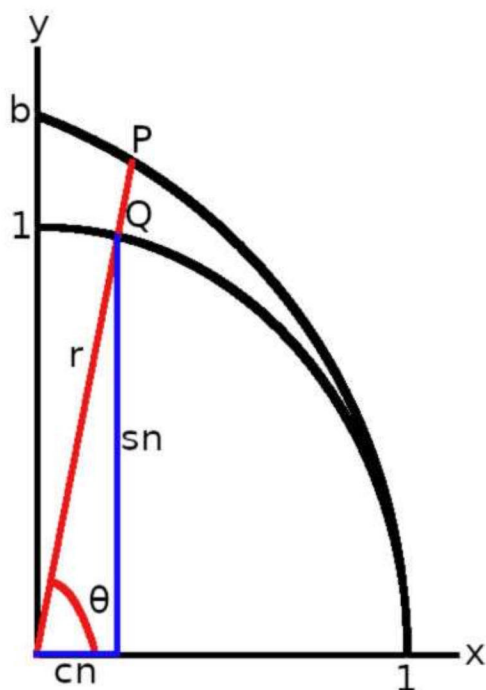


Figure 2.1: The Jacobi Ellipse with  $a = 1$ . The point  $P = (x, y)$  on the ellipse projects onto the unit circle to point  $Q = (cn, sn)$ .

The relationship between elliptic integrals, elliptic functions, and trigonometry is made more clear using arguments from Wikipedia [34]. The standard equation of the unit circle is replaced in the elliptic case by two equations

$$\frac{x^2}{a^2} + \frac{y^2}{b^2} = 1, \tag{2.4}$$

$$x^2 + y^2 = r^2. \tag{2.5}$$

Now we construct the relations

$$sn = \frac{y}{r}, \quad cn = \frac{x}{r}, \quad dn = \frac{1}{r}, \tag{2.6}$$

in order to parameterize an ellipse. Note that figure 2.1 normalizes the ellipse along the x-axis as in [34]. Schwalm [30] uses the other unit ellipse, and also uses a different

set of relations for the functions. Observe that relations (2.6) satisfy both figure 2.1 and equation (2.5), which are described in a combined form by

$$\begin{aligned}x^2 + y^2 &= r^2 \\r^2 \operatorname{cn}^2 + r^2 \operatorname{sn}^2 &= r^2 \\ \operatorname{cn}^2 + \operatorname{sn}^2 &= 1.\end{aligned}\tag{2.7}$$

We must now break free from standard geometric interpretation of ellipses to accommodate the elliptic modulus. A relationship between the elliptic modulus and the eccentricity of an ellipse may be given by

$$k = \frac{\sqrt{b^2 - a^2}}{b} = \text{eccentricity}.\tag{2.8}$$

Equation (2.8) is found conventionally from the eccentricity of an ellipse that is squeezed along the  $y$  axis. We will use this relationship for any elliptic shape we desire since it is just a geometric tool with no real analytic impact. This makes some sense from the perspective that our coordinate system must not only be consistent with the shape of the ellipse, but also the single valued elliptic functions. Relations (2.6) and equations (2.5) to (2.8) lead us to the identity

$$\begin{aligned}x^2 + \frac{y^2}{b^2} &= 1 \\ \operatorname{cn}^2 r^2 + \frac{r^2 \operatorname{sn}^2}{b^2} &= 1 \\ \operatorname{cn}^2 + \frac{\operatorname{sn}^2}{b^2} &= \frac{1}{r^2} \\ 1 - \operatorname{sn}^2 + \frac{\operatorname{sn}^2}{b^2} &= \operatorname{dn}^2 \\ 1 - \operatorname{sn}^2 \left(1 - \frac{1}{b^2}\right) &= \operatorname{dn}^2 \\ 1 - k^2 \operatorname{sn}^2 &= \operatorname{dn}^2\end{aligned}\tag{2.9}$$

Equations (2.7) and (2.9) form the basis for all Jacobi elliptic function square identities. With  $a < b$ , you have  $0 < k^2 < 1$ , which is an ellipse with the major axis along the  $y$  axis. While  $b < a$  gives  $k^2 < 0$ , which is an ellipse with the major axis

along the  $x$  axis. However, the use of the Jacobi elliptic functions includes all elliptic shapes, and not just closed ellipses.

We now push the eccentricity even further by considering  $b$  to be a purely imaginary complex number. Equation (2.8) with imaginary  $b$  now tells us that  $k^2 > 1$ . This choice with equation (2.4) describes geometrically a hyperbola. We now have an understanding of the possible shapes that the Jacobi elliptic functions describe with a real elliptic parameter. It's important to note that a complex  $k^2$  in general leads to a complex torus that does not necessarily have any nice geometrical properties.

Thus far we have purposefully ignored any discussion related to a geometric interpretation of the elliptic function argument  $u$ . We consider a point on an ellipse labelled by  $P = (x, y) = (r \cos \theta, r \sin \theta)$ , which satisfies equation (2.5). Without loss of generality consider a unit ellipse with eccentricity given by

$$x^2 + \frac{y^2}{b^2} = 1 \quad k = \frac{\sqrt{b^2 - 1}}{b}. \quad (2.10)$$

Inserting our point  $P$  into the ellipse of equation (2.10) gives

$$\begin{aligned} r^2 \left( \cos^2 \theta + \frac{\sin^2 \theta}{b^2} \right) &= 1 \\ r^2 \left( 1 - \sin^2 \theta + \frac{\sin^2 \theta}{b^2} \right) &= 1 \\ r^2 \left( 1 - \left( 1 - \frac{1}{b^2} \right) \sin^2 \theta \right) &= 1 \\ r^2 (1 - k^2 \sin^2 \theta) &= 1 \\ r &= \frac{1}{\sqrt{(1 - k^2 \sin^2 \theta)}}. \end{aligned} \quad (2.11)$$

This process leads us full circle back to the elliptic integral of the first kind given by

$$\begin{aligned} u &= \int_0^\theta r(\theta') d\theta' \\ &= \int_0^\theta \frac{d\theta'}{\sqrt{(1 - k^2 \sin^2 \theta')}}. \end{aligned} \quad (2.12)$$

We have effectively defined the elliptic function argument  $u$  from where we started with the trigonometric arguments. It's important to understand how unique equation (2.12) is from standard vector calculus since it has no physical meaning such as area or arc length [30]. The trigonometric arguments are fun and often useful for the sake of intuition towards elliptic functions, but analytically we will push them far from where trigonometry resides. It is extremely important to remember that the Jacobi elliptic functions are defined in general from the inversion of the elliptic integral of the first kind, and not the preceding trigonometric arguments.

The derivatives and integrals of Jacobi elliptic functions behave very similarly to the standard trigonometric functions as well. Equations (2.13) to (2.15) give three useful examples of derivatives of Jacobi elliptic functions.

$$\frac{d}{du} \operatorname{sn} u = \operatorname{cn} u \operatorname{dn} u \quad (2.13)$$

$$\frac{d}{du} \operatorname{cn} u = -\operatorname{sn} u \operatorname{dn} u \quad (2.14)$$

$$\frac{d}{du} \operatorname{dn} u = -k^2 \operatorname{sn} u \operatorname{cn} u \quad (2.15)$$

A few basic integrals of the elliptic functions are given by equations (2.16) to (2.18).

$$\int \operatorname{sn} u \, du = \frac{1}{k} \ln(\operatorname{dn} u - k \operatorname{cn} u) + \text{constant} \quad (2.16)$$

$$\int \operatorname{cn} u \, du = \frac{1}{k} \arccos(\operatorname{dn} u) + \text{constant} \quad (2.17)$$

$$\int \operatorname{dn} u \, du = \arcsin(\operatorname{sn} u) + \text{constant} \quad (2.18)$$

The elliptic functions and integrals of Jacobi are in a way a generalization of the trigonometric functions. They arise often in physics, so naturally it helps to motivate intuitive and familiar definitions where possible. There are many other elliptic functions, but lots of them have no possibility of being explained using any easy trigonometric arguments.

## 2.3 The Weierstrass Elliptic Function

The elliptic function of Weierstrass  $\wp(z)$  is given by

$$\wp(z) = \frac{1}{z^2} + \sum'_{m,n} \frac{1}{(z - 2mw_1 - 2nw_2)^2} - \frac{1}{(2mw_1 + 2nw_2)^2}. \quad (2.19)$$

The summation is taken over all integers except for when both indices are zero. The numbers  $w_1$  and  $w_2$  are the fundamental half-periods of the elliptic function, and their ratio is not real. The Weierstrass elliptic function solves the inversion of the integral

$$z = \int_{\wp(z)}^{\infty} \frac{dx}{\sqrt{4x^3 - g_2x - g_3}}. \quad (2.20)$$

The invariants  $g_2$  and  $g_3$  are related to the roots of the cubic in

$$f(x) = 4x^3 - g_2x - g_3 = 4(x - e_1)(x - e_2)(x - e_3). \quad (2.21)$$

Since equation (2.21) is cubic the relationship between all  $g_i$  and  $e_j$  is laid out by relations

$$e_1 + e_2 + e_3 = 0, \quad e_1e_2 + e_1e_3 + e_2e_3 = -\frac{1}{4}g_2, \quad e_1e_2e_3 = \frac{1}{4}g_3. \quad (2.22)$$

The nonlinear ordinary differential equation

$$\left(\frac{du}{dx}\right)^2 = 4u^3 - g_2u - g_3 \quad (2.23)$$

is solved by the Weierstrass elliptic function.

There exists a theorem by Biermann and Weierstrass that extends the usefulness of this elliptic function even further.

**Theorem (Biermann-Weierstrass):** *Consider the integral*

$$z = \int_a^x \frac{dt}{\sqrt{f(t)}} \quad (2.24)$$

where

$$f(x) \stackrel{\text{def}}{=} a_0x^4 + 4a_1x^3 + 6a_2x^2 + 4a_3x + a_4 \quad (2.25)$$

has no repeated roots; and let its invariants be

$$\begin{aligned} g_2 &\stackrel{\text{def}}{=} a_0 a_4 - 4a_1 a_3 + 3a_2^2 \\ g_3 &\stackrel{\text{def}}{=} a_0 a_2 a_4 + 2a_1 a_2 a_3 - a_2^3 - a_0 a_3^2 - a_1^2 a_4. \end{aligned} \tag{2.26}$$

Then

$$x(z) = a + \frac{\sqrt{f(a)}\wp'(z) + \frac{1}{2}f'(a)\left[\wp(z) - \frac{1}{24}f''(a)\right] + \frac{1}{24}f(a)f'''(a)}{2\left[\wp(z) - \frac{1}{24}f''(a)\right]^2 - \frac{1}{48}f(a)f^{iv}(a)} \tag{2.27}$$

with  $\wp(z) = \wp(z|g_2, g_3)$  [33].

The overwhelming power of the Weierstrass elliptic function should now be strikingly apparent from the preceding theorem. However there does remain a minor “issue” with the Weierstrass elliptic function. On one hand the use of complex numbers does not put any restrictions on our parameter space, though on the other hand there do not exist particularly nice expressions for derivatives or integrals of the function. This can be viewed as an indirect consequence of the Weierstrass function being an analytic tool not motivated at all by elementary functions. However, there do exist particularly nice relationships between the Weierstrass and Jacobi elliptic functions.

We introduce the concept of the modular discriminant for analyzing the two general cases relating the Jacobi and Weierstrass functions. The equation

$$\Delta = g_2^3 - 27g_3^2 \tag{2.28}$$

provides the information we need. It can be identified as the discriminant of equation (2.21). You don’t *need* to go this far, but it can be exploited to keep the elliptic modulus and argument real. For the first case we have  $\Delta > 0$ , and use  $e_1 > 0 \geq e_2 > e_3$ . The relationship

$$\wp(\eta) = e_3 + \frac{e_1 - e_3}{\text{sn}^2(\omega\eta, k)} \tag{2.29}$$

has phase and modulus

$$\omega = \sqrt{e_1 - e_3}, \quad k = \sqrt{\frac{e_2 - e_3}{e_1 - e_3}}. \tag{2.30}$$

Equation (2.29) and relations (2.30) are found in [7] among many other sources. This transformation proves most useful since the Jacobi elliptic functions have nice derivatives and integrals.

The more complicated case of  $\Delta < 0$  can be found in [1]. This case has roots  $e_1 = -\alpha + i\beta$ ,  $e_2 > 0$ , and  $e_3 = \bar{e}_1$ . The constants  $\alpha$  and  $\beta$  satisfy  $\alpha \geq 0$  and  $\beta > 0$ . The relationship

$$\wp(\eta) = e_2 + H_2 \frac{1 + \operatorname{cn}(\omega\eta, k)}{1 - \operatorname{cn}(\omega\eta, k)} \quad (2.31)$$

has phase and modulus

$$\omega = 2\sqrt{H_2}, \quad k = \sqrt{\frac{1}{2} - \frac{3e_2}{4H_2}}, \quad (2.32)$$

where  $H_2$  is equivalent to

$$H_2 = i\sqrt{-H_2^2}, \quad H_2^2 = 3e_2^2 - \frac{g_2}{4}. \quad (2.33)$$

We will use this transformation in chapter 3 to some extent. If it arises that  $g_3 < 0$ , then the reduction

$$\wp(z, g_2, g_3) = -\wp(iz, g_2, -g_3) \quad (2.34)$$

may be employed.

The introduction of some elliptic function theory from complex analysis allows one to understand these concepts in a more fundamental context. This unified approach contains all of the ideas from the preceding sections, but in a clean and concise manner.

## 2.4 The Elliptic Functions

**Definition (elliptic function):** *A complex function that is meromorphic and doubly periodic is called an elliptic function.*

The above definition gives a lot more meaning to equation (2.19). Upon inspection one sees that there is one double pole in the Weierstrass elliptic function. It is also

clear that the function is doubly periodic with half periods  $\omega_1$  and  $\omega_2$ . Following these ideas we construct the **fundamental period parallelograms**.

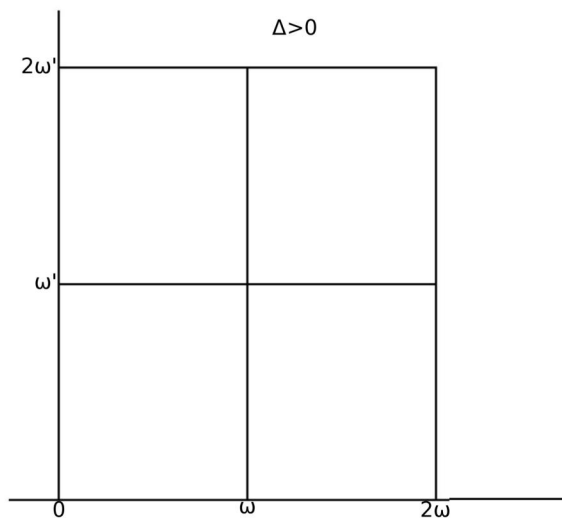


Figure 2.2: The fundamental period parallelogram for the case of  $\Delta > 0$ .

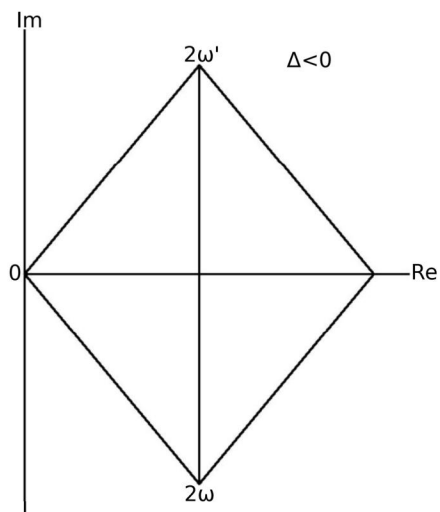


Figure 2.3: The fundamental period parallelogram for the case of  $\Delta < 0$ .

Figures 2.3 and 2.4 give common fundamental rectangles for the Weierstrass elliptic function with the half periods denoted  $\omega$  and  $\omega'$ . The orientation is chosen differently depending on the sign of the discriminant. These fundamental parallelograms may be translated to become an arbitrary **unit cell** without any loss of generality. The Jacobi elliptic functions are constructed by two simple poles as opposed to a single double pole. This difference in pole structure is fundamentally what sets the elliptic functions of Weierstrass and Jacobi apart. They both satisfy the following simple properties.

1. *The number of poles of an elliptic function in any cell is finite.*
2. *The number of zeros of an elliptic function in any cell is finite.*
3. *The sum of the residues of an elliptic function,  $\phi(z)$ , at its poles in any cell is zero.*

Much more could be said about elliptic function theory. Texts such as Whittaker and Watson [33] contain much more information on the subject. It is worth introducing the other functions of Weierstrass that are related to his elliptic function. The derivative of the Weierstrass elliptic function is

$$\wp'(z) = -2 \sum'_{m,n} \frac{1}{(z - 2mw_1 - 2nw_2)^3}. \quad (2.35)$$

The derivative of the Weierstrass elliptic function is also elliptic. Because the Weierstrass elliptic function is even, its derivative is odd. The Weierstrass sigma function is defined by

$$\sigma(z) = z \prod'_{m,n} \left(1 - \frac{z}{2mw_1 + 2nw_2}\right) e^{z/(2mw_1 + 2nw_2) + \frac{1}{2}(z/(2mw_1 + 2nw_2))^2}. \quad (2.36)$$

The sigma function is not an elliptic function, and it is referred to as pseudo periodic instead. The final function of interest is the Weierstrass zeta function given as

$$\zeta(z) = \frac{1}{z} + \sum'_{m,n} \frac{1}{z - 2mw_1 - 2nw_2} + \frac{1}{2mw_1 + 2nw_2} + \frac{z}{(2mw_1 + 2nw_2)^2}. \quad (2.37)$$

Once again the zeta function is not an elliptic function, and is instead pseudo periodic. The Weierstrass zeta function is the logarithmic derivative of the sigma-function, that is,

$$\zeta(z) = \frac{d}{dz} \ln(\sigma(z)). \quad (2.38)$$

The derivative of the zeta function is related to the  $\wp$  function by

$$\frac{d}{dz} \zeta(z) = -\wp(z). \quad (2.39)$$

All four of Weierstrass's functions are formed with invariants  $g_2$  and  $g_3$ . Equations (2.35) to (2.39) are useful when one must do calculus with the Weierstrass elliptic function. The relationships are far less satisfying than those of Jacobi's functions, but they are serviceable. The necessary mathematical background has now been provided. The next chapter will introduce the important physical concepts used in this thesis.

# Chapter 3

## Background: Cosmology

### 3.1 The FLRW Spacetime

Modelling cosmic dynamics involves combining many unique disciplines within physics. The equations and techniques needed for studying the cosmos are vast and depend entirely on what perspective your study is focused. Taking the universe on a massive scale and attempting to approximate its behaviour is one idea. If we can apply the properties of isotropy and homogeneity we arrive at one such model. The sort of size we are talking about here is something like a sphere of radius 100 Mpc [28]. It is thought that at this scale the universe feels the same wherever you are (**homogeneity**) in space, and looks the same wherever you point (**isotropy**). These approximations lead to the FLRW model of the cosmos.

Einstein's field equations of general relativity play a critical role in the quest for understanding spacetime. These equations are very complicated in general, but simplify greatly in certain cases. Special relativity does not include gravity, and has the straightforward spacetime interval given by

$$ds^2 = c^2 dt^2 - dx^2 - dy^2 - dz^2. \quad (3.1)$$

A **spacetime interval** can be thought of as the line element separating events within a spacetime geometry [18]. When gravitation is included we get what is called the

general semi-Riemannian spacetime interval

$$ds^2 = g_{\mu\nu}(x^i)dx^\mu dx^\nu, \quad x^i = (x^0, x^1, x^2, x^3) = (ct, x, y, z), \quad (3.2)$$

where  $g_{\mu\nu}(x^i)$  is called the **metric tensor**, or in some texts it may be referred to as the **metric** instead.

Einstein's equation

$$G_{\mu\nu} - \Lambda g_{\mu\nu} = \frac{8\pi G}{c^4} T_{\mu\nu} \quad (3.3)$$

is what solves for the metric given any distribution of energy-momentum. The Einstein tensor  $G_{\mu\nu}$  contains information about the geometry of spacetime, and the energy-momentum tensor  $T_{\mu\nu}$  contains information about the distribution of *stuff*, matter and energy, throughout the universe. The suspicious term involving  $\Lambda$  brings out the idea of the **cosmological constant**, or **dark energy**. The inclusion of this term may be interpreted in many ways, and the nature of it is still actively studied. Note that this equation hearkens to one of the principles of relativity

$$(\text{the contents of the universe}) = (\text{the geometry of the universe}). \quad (3.4)$$

The FLRW universe has the line element

$$ds^2 = -c^2 dt^2 + a^2(t) [dr^2 + S_\kappa^2(r) d\Omega^2]. \quad (3.5)$$

The coordinate system chosen for equation (3.5) is called **hyper-spherical coordinates** where  $r$  is proportional, but not equal, to the radial distance in general. The factor  $S_\kappa(r)$  depends on whether the universe is spatially flat ( $\kappa = 0$ ), open ( $\kappa = +1$ ), or closed ( $\kappa = -1$ ). The three cases are

$$S_\kappa(r) = \begin{cases} \sin(r) & \kappa = +1 \\ r & \kappa = 0 \\ \sinh(r) & \kappa = -1, \end{cases} \quad (3.6)$$

where  $\kappa$  is called the curvature constant. The factor  $d\Omega$  is just the standard element of solid angle on a 2-sphere

$$d\Omega^2 = d\theta^2 + \sin^2\theta d\phi^2. \quad (3.7)$$

The real intrigue comes with the ever important **scale factor**  $a(t)$ . The expansion or contraction of the universe is mapped by  $a(t)$ , and in general can be a very complicated function with no closed form. We can regard the scale factor as the size of the universe. Note that the units of length are carried by  $a(t)$ , and not the radial coordinate  $r$ .

## 3.2 Distance and Time

There are many different choices for distance and time measures in cosmology. The **proper time** between two events is the elapsed time measured in the reference frame where they occur at the same place. The time on one's own wristwatch is recording their proper time. The **proper distance** between two events is the distance measured in the reference frame where they occur at the same time. These two measures are very important, but not always convenient. Suppose a light signal is sent out from one observer to another. The received signal will be redshifted if the universe is expanding. The **cosmic redshift**  $z$  is given by

$$z = \frac{a(t_{ob}) - a(t_{em})}{a(t_{em})}, \quad (3.8)$$

such that

$$1 + z = \frac{a(t_{ob})}{a(t_{em})}. \quad (3.9)$$

Here  $a(t_{ob})$  is the cosmic scale factor at the time the signal is received, and  $a(t_{em})$  is the cosmic scale factor at the time the signal is emitted. This follows from the definition of radial redshift between two signals

$$1 + z = \frac{\lambda_{ob}}{\lambda_{em}}, \quad (3.10)$$

where  $\lambda$  is wavelength. More details on redshift can be found in Hogg [19].

When we wrote equation (3.5) we used what are called the **comoving coordinates**  $(r, \theta, \phi)$ . These spatial coordinates of cosmological objects do not change with time, and therefore the **comoving distance** is constant with the expansion of the universe. If you consider a purely radial distance between two distant objects

$$ds = a(t) dr, \quad (3.11)$$

then the proper distance may be found by integrating

$$d_p(t) = a(t) r. \quad (3.12)$$

Thus the **recession speed** between the objects at time now  $t_o$

$$v_p(t_o) \stackrel{\text{def}}{=} \dot{d}_p(t_o) \quad (3.13)$$

becomes

$$v_p(t_o) = H_o d_p(t_o), \quad (3.14)$$

where the **Hubble constant**  $H_o$  is the **Hubble parameter**

$$H(t) = \frac{\dot{a}(t)}{a(t)} \quad (3.15)$$

evaluated at time now  $t_o$  [28]. Note that differentiation with a dot is with respect to cosmic proper time  $t$ . Equation (3.14) is a statement of **Hubble's Law**, and is therefore very important. Hubble's Law is the observation that galaxies move away from the earth at a speed proportional to their proper distance.

Sometimes it is not convenient to work with the cosmological proper time  $t$ , as we have done thus far. Consider a photon's trajectory with only radial motion

$$ds^2 = 0 = -c^2 dt^2 + a^2(t) dr^2. \quad (3.16)$$

For a photon emitted at time  $t_e$  and observed today ( $t_o$ ), the radial coordinate is

$$r_o - r_e = -c \int_{t_e}^{t_o} \frac{dt}{a(t)}. \quad (3.17)$$

By convention we set

$$r_o = 0. \tag{3.18}$$

This *null geodesic* leads to a very powerful definition. Let the **conformal time**  $\eta$  be related to the cosmic proper time by

$$c dt \stackrel{\text{def}}{=} a d\eta. \tag{3.19}$$

The distance  $r_e a(t)$  is called the **particle horizon**, and is the furthest proper distance a photon may travel to today from where it was emitted. These ideas of distance and time are only the very basics of cosmology. Further discussion can be found in Ryden [28], Hogg [19], Lineweaver [23], Piattella [25], and many others.

### 3.3 Cosmic Dynamics

We seek to understand how different combinations of matter, dark energy, radiation, and spatial curvature effect the behaviour of an FLRW universe. Friedmann derived the *Friedmann equation*

$$H^2(t) = \frac{8\pi G}{3c^2} \varepsilon(t) + \frac{\Lambda c^2}{3} - \frac{\kappa c^2}{a^2(t)} \tag{3.20}$$

from the Einstein field equations. The third term is related to the spatial curvature of the universe. The energy density of the universe  $\varepsilon(t)$  is unsurprisingly present in equation (3.20) as well. We will need more information in order to properly solve for the expansion history of a given isotropic and homogeneous universe. We define the **critical density**

$$\varepsilon_c(t) = \frac{3c^2}{8\pi G} H^2(t) \tag{3.21}$$

corresponding to a spatially flat universe. Note that the energy density is defined component wise

$$\varepsilon \stackrel{\text{def}}{=} \sum_x \varepsilon_x \tag{3.22}$$

for any  $x$  components. We can thus normalize energy densities accordingly by defining the dimensionless energy density parameter

$$\Omega(t) = \frac{\varepsilon(t)}{\varepsilon_c(t)}. \quad (3.23)$$

If we combine  $\Lambda$  into  $\varepsilon(t)$ , and then rewrite equation (3.20) with dimensionless energy parameters

$$1 - \Omega(t) = -\frac{\kappa c^2}{a^2(t)H^2(t)}. \quad (3.24)$$

Evaluating equation (3.24) at time today leads us to a relationship between the curvature of the universe and its contents

$$\frac{\kappa}{a_o^2} = \frac{H_o^2}{c^2}(\Omega_o - 1). \quad (3.25)$$

The idea is that measuring the curvature of the universe today is probably impossible, but indeed we can find it if we have ideas for  $H_o$  and  $\Omega_o$ .

#### The first law of thermodynamics

$$dQ = dE + PdV \quad (3.26)$$

applied to our expanding universe leads to another equation. Assuming heat does not flow into or out of our universe ( $dQ = 0$ ), we have

$$\dot{E} + P\dot{V} = 0. \quad (3.27)$$

Take the universe to be a sphere of volume

$$V(t) = \frac{4}{3}\pi r_s^3 a^3(t), \quad (3.28)$$

and internal energy

$$E(t) = V(t)\varepsilon(t). \quad (3.29)$$

We now get the **fluid equation**

$$\dot{\varepsilon}(t) + 3\frac{\dot{a}(t)}{a(t)}[\varepsilon(t) + P(t)] = 0. \quad (3.30)$$

The rest of the details can be found in Ryden [28]. The comoving radius of the sphere  $r_s$  has corresponding proper radius

$$R_s = a(t)r_s, \tag{3.31}$$

as seen in equation (3.12). We approximate our universe to be a perfect fluid since we can largely ignore the internal stresses of our cosmological components. This means that the pressure is related linearly to the energy density by the following *equation of state*

$$P(t) = w\varepsilon(t), \tag{3.32}$$

where  $w$  is called the **equation of state parameter**. The value of  $w$  for a particular type of fluid depends on what it is comprised of. The most common types of cosmological fluids are:

$$\text{dust, } w = 0; \tag{3.33}$$

$$\text{radiation, } w = 1/3; \tag{3.34}$$

$$\text{dark energy, } w = -1. \tag{3.35}$$

Here dust is non-relativistic matter, radiation is photons and relativistic matter, and dark energy is the cosmological constant. You sometimes see some alternative theory fluids such as:

$$\text{quintessence, } w = -2/3; \tag{3.36}$$

$$\text{strings, } w = -1/3. \tag{3.37}$$

Modelling information corresponding to quintessence and strings can be found in Steiner [31]. The fluid equation (3.30) together with the Friedmann equation (3.20) forms the **acceleration equation**

$$\frac{\ddot{a}(t)}{a(t)} = -\frac{4\pi G}{3c^2}[\varepsilon(t) + 3P(t)] + \frac{\Lambda c^2}{3}. \tag{3.38}$$

See Ryden [28] for details. The equation of state (3.32) allows us an explicit analytic solution to the fluid equation (3.30)

$$\varepsilon = \varepsilon_o \left( \frac{a}{a_o} \right)^{-3(1+w)}, \quad (3.39)$$

where  $\varepsilon_o$  is just  $\varepsilon(a(t_o))$ , and considered to be the energy density at time now. We have the tools to describe the expansion history of many interesting model universes. We often want to use a dimensionless scale factor such as

$$\tilde{a} = \frac{a}{a_o}. \quad (3.40)$$

This together with the energy density parameters provides the Friedmann equation in dimensionless form

$$\left( \frac{\dot{\tilde{a}}}{\tilde{a}} \right)^2 = \Omega_\Lambda + \frac{\Omega_{m,o}}{\tilde{a}^3} + \frac{\Omega_{r,o}}{\tilde{a}^4} + \frac{\Omega_{c,o}}{\tilde{a}^2}, \quad (3.41)$$

which includes dark energy, matter, radiation, and spatial curvature. Writing Friedmann's equation this way was made possible by having a solved fluid equation. This is commonly known as the generalised  $\Lambda$ CDM model because today's universe is thought to be primarily comprised of dark energy and cold dark matter. The initial density parameters are used to create different model universes assuming some value of  $H_o$ . Equation (3.41) will be of more use to use in terms of conformal time, so using the chain rule of differential calculus

$$\begin{aligned} \frac{1}{\tilde{a}^2} \left( \frac{d\tilde{a}}{dt} \right)^2 &= \Omega_\Lambda + \frac{\Omega_{m,o}}{\tilde{a}^3} + \frac{\Omega_{r,o}}{\tilde{a}^4} + \frac{\Omega_{c,o}}{\tilde{a}^2} \\ \frac{1}{\tilde{a}^2} \left( \frac{d\tilde{a}}{d\eta} \frac{d\eta}{dt} \right)^2 &= \Omega_\Lambda + \frac{\Omega_{m,o}}{\tilde{a}^3} + \frac{\Omega_{r,o}}{\tilde{a}^4} + \frac{\Omega_{c,o}}{\tilde{a}^2} \\ \frac{1}{\tilde{a}^2} \left( \frac{d\tilde{a}}{d\eta} \frac{1}{\tilde{a}} \right)^2 &= \Omega_\Lambda + \frac{\Omega_{m,o}}{\tilde{a}^3} + \frac{\Omega_{r,o}}{\tilde{a}^4} + \frac{\Omega_{c,o}}{\tilde{a}^2} \\ \frac{1}{\tilde{a}^4} \left( \frac{d\tilde{a}}{d\eta} \right)^2 &= \Omega_\Lambda + \frac{\Omega_{m,o}}{\tilde{a}^3} + \frac{\Omega_{r,o}}{\tilde{a}^4} + \frac{\Omega_{c,o}}{\tilde{a}^2} \\ \left( \frac{d\tilde{a}}{d\eta} \right)^2 &= \Omega_\Lambda \tilde{a}^4 + \Omega_{m,o} \tilde{a} + \Omega_{r,o} + \Omega_{c,o} \tilde{a}^2. \end{aligned} \quad (3.42)$$

We write

$$[\tilde{a}'(\eta)]^2 = \Omega_\Lambda [\tilde{a}(\eta)]^4 + \Omega_{c,o} [\tilde{a}(\eta)]^2 + \Omega_{m,o} [\tilde{a}(\eta)] + \Omega_{r,o}. \quad (3.43)$$

Note that differentiation with a prime is with respect to conformal time  $\eta$ .

### 3.4 General Solution for FLRW Scale Factor

This section will finally combine ideas from all of chapters 2 and 3. Special functions are used to solve for an analytical solution to equation (3.43). This will provide a sturdy platform for which my results are obtained.

Let us take a warm up lap before we engage in the real violence of solving equation (3.43) explicitly. There's a fairly simple model universe that will build into something very intriguing in chapter 3. We take our universe to be spatially flat, and to contain only matter and dark energy. The Friedmann equation (3.43) becomes

$$[\tilde{a}'(\eta)]^2 = \Omega_\Lambda [\tilde{a}(\eta)]^4 + \Omega_{m,o} [\tilde{a}(\eta)]. \quad (3.44)$$

Integrating (3.44) we have

$$\frac{a_0 H_o}{c} \eta = \int_0^{\tilde{a}(\eta)} \frac{du}{\sqrt{u(\Omega_{m,o} + \Omega_{m,o} u^3)}}. \quad (3.45)$$

The solution to (3.45) is provided in terms of Jacobi elliptic functions by Sazhin et al [14]

$$\tilde{a}(\eta) = \left( \frac{\Omega_{m,o}}{\Omega_\Lambda} \right)^{1/3} \frac{1 - \text{cn}(\omega\eta, k)}{\sqrt{3}(1 + \text{cn}(\omega\eta, k)) - (1 - \text{cn}(\omega\eta, k))}, \quad (3.46)$$

where the phase and elliptic modulus are

$$\omega = 3^{1/4} \Omega_\Lambda^{1/6} \Omega_{m,o}^{1/3}, \quad k = \frac{\sqrt{2 + \sqrt{3}}}{2}. \quad (3.47)$$

We have a universe that seems to represent ours well if we set  $\Omega_{m,o} = 0.32$ , and  $\Omega_\Lambda = 0.68$  [5].

The addition of radiation and curvature complicates the situation, but not gravely. It might be realistic to add small amounts of radiation and spatial curvature to

models. Some may also find pedagogical significance in many wild combinations of cosmological fluids. Steiner [31] employs the Biermann-Weierstrass theorem (section 2.3) to solve equation (3.43) in terms of Weierstrass elliptic functions. The works of Edwards [10], and D'Ambroise [9] provide other solutions. Following Steiner's [31] approach we have

$$\tilde{a}(\tilde{\eta}) = \frac{\frac{1}{2}\Omega_{m,o}[\wp(\tilde{\eta}) - \frac{1}{12}\Omega_{c,o}] - \sqrt{\Omega_{r,o}}\wp'(\tilde{\eta})}{2[\wp(\tilde{\eta}) - \frac{1}{12}\Omega_{c,o}]^2 - \frac{1}{2}\Omega_{r,o}\Omega_{\Lambda}}, \quad (3.48)$$

where

$$\wp(\tilde{\eta}) \stackrel{\text{def}}{=} \wp(\tilde{\eta}|g_2, g_3), \quad (3.49)$$

with

$$g_2 = \Omega_{\Lambda}\Omega_{r,o} + \frac{1}{12}\Omega_{c,o}^2, \quad g_3 = \frac{1}{6}\Omega_{\Lambda}\Omega_{r,o}\Omega_{c,o} - \frac{1}{16}\Omega_{\Lambda}\Omega_{m,o}^2 - \frac{1}{216}\Omega_{c,o}^3. \quad (3.50)$$

The argument  $\tilde{\eta}$  is the rescaled conformal time

$$\tilde{\eta} = \frac{a_o H_o}{c} \eta. \quad (3.51)$$

When dark energy is included in this model there may be a finite limit to conformal time such that the scale factor  $a \rightarrow \infty$  as  $\eta \rightarrow \eta_{\infty}$ . Steiner [31] provides a crafty way to calculate this limit using

$$\wp(\tilde{\eta}_{\infty}) = \frac{1}{2}\sqrt{\Omega_{r,o}\Omega_{\Lambda}} + \frac{1}{12}\Omega_{c,o} \quad (3.52)$$

or

$$\wp'(\tilde{\eta}_{\infty}) = -\frac{1}{4}\Omega_{m,o}\sqrt{\Omega_{\Lambda}}. \quad (3.53)$$

More limiting expressions and values may be found in Steiner's paper [31].

The results of this section will serve as the primary framework for this thesis to be built upon. Equations (3.46) and (3.48) provide the opportunity to calculate and plot a wealth of physically important quantities. The nature of elliptic functions and integrals also allows for great mathematical discussion. We have acquired the necessary and sufficient background to move on to results.

# Chapter 4

## Results

### 4.1 Model Solutions

The general result of equation (3.48) has a remarkably simple form. The introduction of conformal time has allowed for such a solution to exist. Actually the conformal time plays the role of what's called a *uniformizing variable* of the mathematical equation

$$y^2 = A_0x^4 + A_1x^3 + A_2x^2 + A_3x + A_4, \quad (4.1)$$

which has lead to the general solution of the scale factor. This is worth noting because although  $x$  is a four-valued function of  $y$ , and  $y$  is a two-valued function of  $x$ ;  $x$  and  $y$  are one-valued functions of conformal time  $\eta$  [33].

A fairly annoying problem does exist with the modelling described thus far. We do not have the ability to calculate cosmological proper time in terms of conformal time. This is an issue because it would be very convenient to have a parametric model that includes both  $a(\eta)$  and  $t(\eta)$ . This would allow for a more comprehensive overview of Friedmann models. From the definition of conformal time we form the integral

$$t(\eta) = \frac{1}{c} \int_0^\eta a(\eta') d\eta'. \quad (4.2)$$

We introduce dimensionless proper time,

$$\tilde{t} = H_o t \quad (4.3)$$

and with our dimensionless and rescaled variables  $\tilde{t}$ ,  $\tilde{\eta}$ , and  $\tilde{a}$  we write

$$\tilde{t}(\tilde{\eta}) = \int_0^{\tilde{\eta}} \tilde{a}(\tilde{\eta}') d\tilde{\eta}'. \quad (4.4)$$

Calculating the integral in equation (4.4) would be one such way to solve for a parametric model of scale factor and proper time. It's important to remember that this is all within the context of having the parameters  $H_o$ ,  $\Omega_\Lambda$ ,  $\Omega_{m,o}$ , and  $\Omega_{r,o}$ . The choice of these parameters has great impact on what form the solution takes. The next section will begin the approach to solving for proper time as a function of conformal time.

## 4.2 The Spatially-Flat $\Lambda$ CDM Model

An important special case of the FLRW universe is where we have only matter (baryonic and cold dark) and dark energy (the cosmological constant), that is to say,  $\Omega_{c,o} = \Omega_{r,o} = 0$ . It is predicted by both the WMAP probe [24] and more recently the Planck Collaboration [5] that the universe is primarily comprised of only these two substances. The equations still involve elliptic functions despite the simplicity. Equation (3.48) simplifies to

$$\tilde{a}(\tilde{\eta}) = \frac{\Omega_{m,o}}{4\wp(\tilde{\eta})}, \quad (4.5)$$

where the invariants of  $\wp(\tilde{\eta})$  are

$$g_2 = 0, \quad g_3 = -\frac{1}{16}\Omega_\Lambda\Omega_{m,o}^2. \quad (4.6)$$

This may be converted to Jacobi elliptic functions as in equation (3.46).

Surprisingly there is a well known solution for  $a(t)$  in this case. This solution also has the nice property of being invertible so that  $t(a)$  may also be explicitly given. The form used by Ryden [28] reads

$$\tilde{t}(\tilde{a}) = \frac{2}{3\sqrt{\Omega_\Lambda}} \ln \left[ \left( \frac{\Omega_\Lambda}{\Omega_{m,o}} \right)^{3/2} \tilde{a}^{3/2} + \sqrt{1 + \left( \frac{\Omega_\Lambda}{\Omega_{m,o}} \right) \tilde{a}^3} \right]. \quad (4.7)$$

This allows one to insert an expression for  $a(\eta)$  to obtain  $t(\eta)$ . Inserting equation (4.5) into equation (3.7) leads to

$$\tilde{t}(\tilde{\eta}) = \frac{2}{3\sqrt{\Omega_\Lambda}} \ln \left[ \frac{1}{8} \Omega_{m,o} \sqrt{\Omega_\Lambda} [\wp(\tilde{\eta})]^{-3/2} + \sqrt{1 + \frac{1}{64} \Omega_{m,o}^2 \Omega_\Lambda [\wp(\tilde{\eta})]^{-3}} \right]. \quad (4.8)$$

Thus we complete a parametric solution determining the expansion history for the flat  $\Lambda$ CDM model.

Up to this point nothing new has been done. Another way to find an equivalent flat  $\Lambda$ CDM solution is by solving the integral in equation (4.4). We write

$$\tilde{t}(\tilde{\eta}) = \frac{\Omega_{m,o}}{4} \int_0^{\tilde{\eta}} \frac{d\tilde{\eta}'}{\wp(\tilde{\eta}')}, \quad (4.9)$$

and recognize that this can be solved from the formula

$$\wp'(v) \int \frac{du}{\wp(u) - \wp(v)} = \log \left[ \frac{\sigma(u-v)}{\sigma(u+v)} \right] + 2u\zeta(v) \quad (4.10)$$

provided by Abramowitz and Stegun [1]. Since equation (3.52) in this case reads  $\wp(\tilde{\eta}_\infty) = 0$  we may write

$$\tilde{t}(\tilde{\eta}) = \frac{\Omega_{m,o}}{4} \int_0^{\tilde{\eta}} \frac{d\tilde{\eta}'}{\wp(\tilde{\eta}') - \wp(\tilde{\eta}_\infty)} \quad (4.11)$$

$$\tilde{t}(\tilde{\eta}) = -\frac{1}{\sqrt{\Omega_\Lambda}} \left\{ \ln \left| \frac{\sigma(\tilde{\eta} - \tilde{\eta}_\infty)}{\sigma(\tilde{\eta} + \tilde{\eta}_\infty)} \right| + 2\tilde{\eta}\zeta(\tilde{\eta}_\infty) \right\}, \quad (4.12)$$

where equation 2.90 has also been used. Equation (4.12) is a special case of a solution given by Lemaître [21, 22].

It's not clear how equations (4.12) and (4.8) are related. One might expect that some identities could be used to prove that they are equivalent. Attempts at this have been unsuccessful thus far, but that does not mean that they are not the same to some degree. It's reasonable to believe that equations (4.12) and (3.8) are at least equal in the physically significant region  $\eta \in (0, \eta_\infty)$ . This is based on the simple assumption that no incorrect mathematical formulae have been applied in either case.

For an example we consider a universe with parameters  $\Omega_\Lambda = 0.6847$ ,  $\Omega_{m,o} = 0.3153$ , and  $H_o = 67.36 \text{ km s}^{-1} \text{ Mpc}^{-1}$  provided by Planck [5]. We compare results from equations (3.12) and (3.8) with a purely numerical solution.

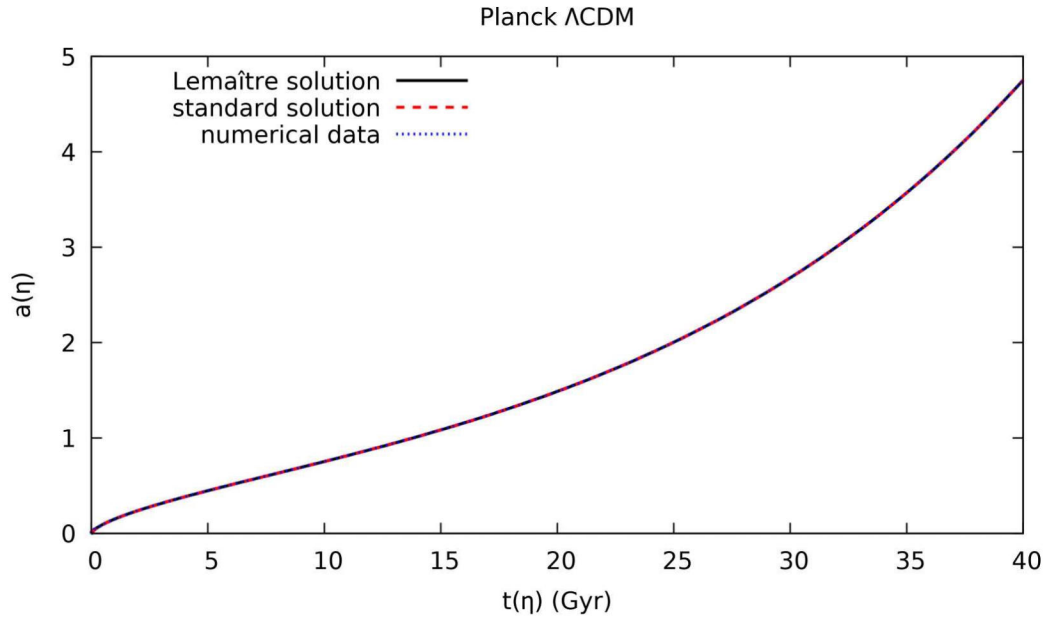


Figure 4.1: Three methods for plotting the Planck universe. Equation (4.12) is the *Lemaître solution*, equation (4.8) is the *standard solution*, and finally a *numerical solution* curve is shown as a sanity check.

Indeed both equations (4.12) and (4.8) produce indistinguishable data and therefore bear some equivalence. Planck [5] lists the age of the universe as 13.797 Gyr. The data from figure 4.1 is very close at 13.802 Gyr. This difference is extremely small, and it falls well within the error bars provided by Planck’s data. The significance of this should be taken with a grain of salt. The data provided by Planck [5] is extremely sophisticated, and is only being used for a basic demonstration.

### 4.3 The Hyperelliptic Integral Method

Thus far all discussion has been focused on the functions of Weierstrass. It would be reasonable to instead convert equation (3.48) into Jacobi elliptic functions, and then integrate. We look at the matter and dark energy only universe again as an example. The modular discriminant provided by equation (2.28) is negative for this case. Thus the transformation formula will be equation (2.31) with the appropriate choice of  $e_1$ ,  $e_2$ , and  $e_3$ . We need  $H_2$ , which is just related to  $e_2$  in this case

$$H_2 = -\sqrt{3}e_2. \quad (4.13)$$

Now the elliptic modulus is simply

$$k = \sqrt{\frac{1}{2} - \frac{3e_2}{4H_2}} = \frac{\sqrt{2 + \sqrt{3}}}{2}. \quad (4.14)$$

Invoking the transformation equation (2.34) let's us write the  $\wp$  function as

$$\wp(\tilde{\eta}) = e_2 \left[ \frac{-(1 - \text{cn}(\hat{\omega}\tilde{\eta}, k)) + \sqrt{3}(1 + \text{cn}(\hat{\omega}\tilde{\eta}, k))}{1 - \text{cn}(\hat{\omega}\tilde{\eta}, k)} \right], \quad (4.15)$$

with a real phase  $\hat{\omega}$

$$\hat{\omega} = 2H_2^{1/2} = 3^{1/4}e_2^{1/2}. \quad (4.16)$$

What's left is to solve for  $e_2$  and write down the scale factor. The modular invariants are

$$\begin{aligned} g_2 &= 0 \\ g_3 &= -\frac{1}{16}\Omega_\Lambda\Omega_{m,o}^2. \end{aligned} \quad (4.17)$$

The cubic of (2.21) now gives

$$e_2 = \frac{1}{4}\Omega_\Lambda^{1/3}\Omega_{m,o}^{2/3}. \quad (4.18)$$

After a little algebra we write equation (4.5) as

$$\tilde{a}(\tilde{\eta}) = \left( \frac{\Omega_{m,o}}{\Omega_\Lambda} \right)^{1/3} \frac{1 - \text{cn}(\hat{\omega}\tilde{\eta}, k)}{\sqrt{3}(1 + \text{cn}(\hat{\omega}\tilde{\eta}, k)) - (1 - \text{cn}(\hat{\omega}\tilde{\eta}, k))}, \quad (4.19)$$

which has employed equations (4.15) and (4.18). The phase and elliptic modulus are

$$\hat{\omega} = 3^{1/4} \Omega_\Lambda^{1/6} \Omega_{m,o}^{1/3} \quad k = \frac{\sqrt{2 + \sqrt{3}}}{2}. \quad (4.20)$$

This is just equations (3.46) and (3.47), which are already known. To integrate equation (4.19) it would be convenient to break it up a little. Partial fractions yield

$$\tilde{a}(\tilde{\eta}) = \left( \frac{\Omega_{m,o}}{\Omega_\Lambda} \right)^{1/3} \left( \frac{\sqrt{3}}{1 + \gamma \operatorname{cn}(\hat{\omega} \tilde{\eta}, k)} - \frac{1}{\sqrt{3} + 1} \right), \quad (4.21)$$

where

$$\gamma = \frac{(\sqrt{3} + 1)^2}{2}. \quad (4.22)$$

The integral equation (4.4) is now

$$\tilde{t}(\tilde{\eta}) = \left( \frac{\Omega_{m,o}}{\Omega_\Lambda} \right)^{1/3} \int_0^{\tilde{\eta}} \left( \frac{\sqrt{3}}{1 + \gamma \operatorname{cn}(\hat{\omega} \tilde{\eta}', k)} - \frac{1}{\sqrt{3} + 1} \right) d\tilde{\eta}'. \quad (4.23)$$

We split up the integral equation (4.23) as

$$\tilde{t}(\tilde{\eta}) = J_1 + J_2, \quad (4.24)$$

where we have a rather hard integral

$$J_1 = \left( \frac{\Omega_{m,o}}{\Omega_\Lambda} \right)^{1/3} \int_0^{\tilde{\eta}} \frac{\sqrt{3}}{1 + \gamma \operatorname{cn}(\hat{\omega} \tilde{\eta}', k)} d\tilde{\eta}', \quad (4.25)$$

and a very easy integral

$$J_2 = - \left( \frac{\Omega_{m,o}}{\Omega_\Lambda} \right)^{1/3} \int_0^{\tilde{\eta}} \frac{1}{\sqrt{3} + 1} d\tilde{\eta}'. \quad (4.26)$$

The integral  $J_2$  is trivial

$$J_2 = - \left( \frac{\Omega_{m,o}}{\Omega_\Lambda} \right)^{1/3} \frac{1}{\sqrt{3} + 1} \tilde{\eta}, \quad (4.27)$$

but  $J_1$  poses serious problems. Byrd and Friedman [2] unfortunately do not have quite the correct solution for  $J_1$ . However, the authors do provide sufficient tools for treating hyperelliptic integrals regardless. The square identity

$$\operatorname{cn}^2(\phi, k) = 1 - \operatorname{sn}^2(\phi, k) \quad (4.28)$$

can be used to split up  $J_1$

$$J_1 = \left( \frac{\Omega_{m,o}}{\Omega_\Lambda} \right)^{1/3} \frac{\sqrt{3}}{1 - \gamma^2} \left[ \int_0^{\tilde{\eta}} \frac{1}{1 - \frac{\gamma^2}{\gamma^2 - 1} \text{sn}(\hat{\omega}\tilde{\eta}', k)^2} d\tilde{\eta}' \right. \\ \left. - \gamma \int_0^{\tilde{\eta}} \frac{\text{cn}(\hat{\omega}\tilde{\eta}', k)}{1 - \frac{\gamma^2}{\gamma^2 - 1} \text{sn}(\hat{\omega}\tilde{\eta}', k)^2} d\tilde{\eta}' \right]. \quad (4.29)$$

Consider the case  $\tilde{\eta} \leq \frac{1}{\hat{\omega}} \text{sn}^{-1}(1, k)$ . We want to write  $J_1$  in Legendre form to find the solution, and thus we need a suitable substitution. We note that  $\text{sn}(\hat{\omega}\tilde{\eta}', k)$ ,  $\text{dn}(\hat{\omega}\tilde{\eta}', k)$ , and  $\text{cn}(\hat{\omega}\tilde{\eta}', k)$  are all positive in the current regime. The substitution

$$u = \text{sn}(\hat{\omega}\tilde{\eta}', k) \\ du = \hat{\omega} \text{cn}(\hat{\omega}\tilde{\eta}', k) \text{dn}(\hat{\omega}\tilde{\eta}', k) d\tilde{\eta}' \\ \text{cn}(\hat{\omega}\tilde{\eta}', k) = \sqrt{1 - \text{sn}(\hat{\omega}\tilde{\eta}', k)^2} \\ \text{dn}(\hat{\omega}\tilde{\eta}', k) = \sqrt{1 - k^2 \text{sn}(\hat{\omega}\tilde{\eta}', k)^2} \\ d\tilde{\eta}' = \frac{du}{\hat{\omega} \sqrt{(1 - u^2)} \sqrt{(1 - k^2 u^2)}} \quad (4.30)$$

may therefore be employed. This leads to the following integrals

$$J_1 = \left( \frac{\Omega_{m,o}}{\Omega_\Lambda} \right)^{1/3} \frac{\sqrt{3}}{1 - \gamma^2} \frac{1}{\hat{\omega}} \left[ \int_0^{u_1} \frac{1}{(1 - \frac{\gamma^2}{\gamma^2 - 1} u^2) \sqrt{(1 - u^2)} \sqrt{(1 - k^2 u^2)}} du \right. \\ \left. - \gamma \int_0^{u_1} \frac{1}{(1 - \frac{\gamma^2}{\gamma^2 - 1} u^2) \sqrt{(1 - k^2 u^2)}} du \right], \quad (4.31)$$

where  $u_1 = \text{sn}(\hat{\omega}\tilde{\eta}, k)$ . The integral  $J_1$  has solution

$$J_1 = \left( \frac{\Omega_{m,o}}{\Omega_\Lambda} \right)^{1/3} \frac{\sqrt{3}}{1 - \gamma^2} \frac{1}{\hat{\omega}} \left\{ \Pi \left( \text{sn}(\hat{\omega}\tilde{\eta}, k), \frac{\gamma^2}{\gamma^2 - 1}, k \right) \right. \\ \left. - \frac{\gamma}{2} \sqrt{\frac{\gamma^2 - 1}{\gamma^2 k'^2 + k^2}} \left[ \ln \left( \frac{\sqrt{\gamma^2 - 1} \text{dn}(\hat{\omega}\tilde{\eta}, k) + \sqrt{\gamma^2 k^2 + k^2 \text{sn}(\hat{\omega}\tilde{\eta}, k)}}{\sqrt{\gamma^2 - 1} \text{dn}(\hat{\omega}\tilde{\eta}, k) - \sqrt{\gamma^2 k^2 + k^2 \text{sn}(\hat{\omega}\tilde{\eta}, k)}} \right) - i\pi \right] \right\}. \quad (4.32)$$

This is where the hyperelliptic method becomes more interesting. The value of  $u_1$  reaches a maximum of 1, and then decreases back to 0. This is true because the arguments  $k$ ,  $\hat{\omega}$  and  $\tilde{\eta}$  are all real. This is an issue because  $\text{cn}(\hat{\omega}\tilde{\eta}, k)$  actually becomes

negative in this regime. This means that in the case  $\tilde{\eta} \geq \frac{1}{\hat{\omega}} \text{sn}^{-1}(1, k)$  we change the substitution to

$$\begin{aligned}
u &= \text{sn}(\hat{\omega}\tilde{\eta}', k) \\
du &= \hat{\omega} \text{cn}(\hat{\omega}\tilde{\eta}', k) \text{dn}(\hat{\omega}\tilde{\eta}', k) d\tilde{\eta}' \\
\text{cn}(\hat{\omega}\tilde{\eta}', k) &= -\sqrt{1 - \text{sn}(\hat{\omega}\tilde{\eta}', k)^2} \\
\text{dn}(\hat{\omega}\tilde{\eta}', k) &= \sqrt{1 - k^2 \text{sn}(\hat{\omega}\tilde{\eta}', k)^2} \\
d\tilde{\eta}' &= -\frac{du}{\hat{\omega} \sqrt{(1-u^2)} \sqrt{(1-k^2u^2)}}.
\end{aligned} \tag{4.33}$$

Now  $J_1$  splits up as

$$\begin{aligned}
J_1 &= \left(\frac{\Omega_{m,o}}{\Omega_\Lambda}\right)^{1/3} \frac{\sqrt{3}}{1-\gamma^2} \frac{1}{\hat{\omega}} \left[ \int_0^1 \frac{1}{(1-\frac{\gamma^2}{\gamma^2-1}u^2)\sqrt{(1-u^2)}\sqrt{(1-k^2u^2)}} du \right. \\
&\quad - \int_1^{u_1} \frac{1}{(1-\frac{\gamma^2}{\gamma^2-1}u^2)\sqrt{(1-u^2)}\sqrt{(1-k^2u^2)}} du \\
&\quad \left. - \gamma \int_0^{u_1} \frac{1}{(1-\frac{\gamma^2}{\gamma^2-1}u^2)\sqrt{(1-k^2u^2)}} du \right],
\end{aligned} \tag{4.34}$$

which is really just

$$\begin{aligned}
J_1 &= \left(\frac{\Omega_{m,o}}{\Omega_\Lambda}\right)^{1/3} \frac{\sqrt{3}}{1-\gamma^2} \frac{1}{\hat{\omega}} \left[ 2 \int_0^1 \frac{1}{(1-\frac{\gamma^2}{\gamma^2-1}u^2)\sqrt{(1-u^2)}\sqrt{(1-k^2u^2)}} du \right. \\
&\quad - \int_0^{u_1} \frac{1}{(1-\frac{\gamma^2}{\gamma^2-1}u^2)\sqrt{(1-u^2)}\sqrt{(1-k^2u^2)}} du \\
&\quad \left. - \gamma \int_0^{u_1} \frac{1}{(1-\frac{\gamma^2}{\gamma^2-1}u^2)\sqrt{(1-k^2u^2)}} du \right].
\end{aligned} \tag{4.35}$$

The solution of  $J_1$  in this case is

$$\begin{aligned}
J_1 &= \left(\frac{\Omega_{m,o}}{\Omega_\Lambda}\right)^{1/3} \frac{\sqrt{3}}{1-\gamma^2} \frac{1}{\hat{\omega}} \left\{ 2\Pi\left(\frac{\gamma^2}{\gamma^2-1}, k\right) - \Pi\left(\text{sn}(\hat{\omega}\tilde{\eta}, k), \frac{\gamma^2}{\gamma^2-1}, k\right) \right. \\
&\quad \left. - \frac{\gamma}{2} \sqrt{\frac{\gamma^2-1}{\gamma^2k'^2+k^2}} \left[ \ln\left(\frac{\sqrt{\gamma^2-1}\text{dn}(\hat{\omega}\tilde{\eta}, k) + \sqrt{\gamma^2k^2+k^2}\text{sn}(\hat{\omega}\tilde{\eta}, k)}{\sqrt{\gamma^2-1}\text{dn}(\hat{\omega}\tilde{\eta}, k) - \sqrt{\gamma^2k^2+k^2}\text{sn}(\hat{\omega}\tilde{\eta}, k)}\right) - i\pi \right] \right\}.
\end{aligned} \tag{4.36}$$

Now putting everything together we have

$$\begin{aligned} \tilde{t}(\tilde{\eta}) = & \left( \frac{\Omega_{m,o}}{\Omega_\Lambda} \right)^{1/3} \frac{\sqrt{3}}{1-\gamma^2} \frac{1}{\hat{\omega}} \left\{ \Pi \left( \operatorname{sn}(\hat{\omega}\tilde{\eta}, k), \frac{\gamma^2}{\gamma^2-1}, k \right) \right. \\ & - \frac{\gamma}{2} \sqrt{\frac{\gamma^2-1}{\gamma^2 k'^2 + k^2}} \left[ \ln \left( \frac{\sqrt{\gamma^2-1} \operatorname{dn}(\hat{\omega}\tilde{\eta}, k) + \sqrt{\gamma^2 k^2 + k^2} \operatorname{sn}(\hat{\omega}\tilde{\eta}, k)}{\sqrt{\gamma^2-1} \operatorname{dn}(\hat{\omega}\tilde{\eta}, k) - \sqrt{\gamma^2 k^2 + k^2} \operatorname{sn}(\hat{\omega}\tilde{\eta}, k)} \right) - i\pi \right] \\ & \left. - \frac{1}{\sqrt{3}+1} \tilde{\eta} \right\}, \quad \tilde{\eta} \leq \frac{1}{\hat{\omega}} \operatorname{sn}^{-1}(1, k), \end{aligned} \quad (4.37)$$

and

$$\begin{aligned} \tilde{t}(\tilde{\eta}) = & \left( \frac{\Omega_{m,o}}{\Omega_\Lambda} \right)^{1/3} \frac{\sqrt{3}}{1-\gamma^2} \frac{1}{\hat{\omega}} \left\{ 2\Pi \left( \frac{\gamma^2}{\gamma^2-1}, k \right) - \Pi \left( \operatorname{sn}(\hat{\omega}\tilde{\eta}, k), \frac{\gamma^2}{\gamma^2-1}, k \right) \right. \\ & - \frac{\gamma}{2} \sqrt{\frac{\gamma^2-1}{\gamma^2 k'^2 + k^2}} \left[ \ln \left( \frac{\sqrt{\gamma^2-1} \operatorname{dn}(\hat{\omega}\tilde{\eta}, k) + \sqrt{\gamma^2 k^2 + k^2} \operatorname{sn}(\hat{\omega}\tilde{\eta}, k)}{\sqrt{\gamma^2-1} \operatorname{dn}(\hat{\omega}\tilde{\eta}, k) - \sqrt{\gamma^2 k^2 + k^2} \operatorname{sn}(\hat{\omega}\tilde{\eta}, k)} \right) - i\pi \right] \\ & \left. - \frac{1}{\sqrt{3}+1} \tilde{\eta} \right\}, \quad \tilde{\eta} \geq \frac{1}{\hat{\omega}} \operatorname{sn}^{-1}(1, k). \end{aligned} \quad (4.38)$$

Equations (4.37) and (4.38) are certainly a lot more cumbersome than equation (4.12). It's possible to generalise this method to include radiation and spatial curvature, but doing so would be rather sinful. In the next section we will use the functions of Weierstrass to do the same task with much less effort.

It is still interesting to make sure equations (4.37) and (4.38) agree with our work from the previous sections of this chapter. Consider two initial states where the first has dimensionless energy parameters  $\Omega_{m,o} = 0.10$  and  $\Omega_\Lambda = 0.90$ . The second we choose to have  $\Omega_{m,o} = 0.90$  and  $\Omega_\Lambda = 0.10$ . We use equation (4.12) to benchmark the new expression.

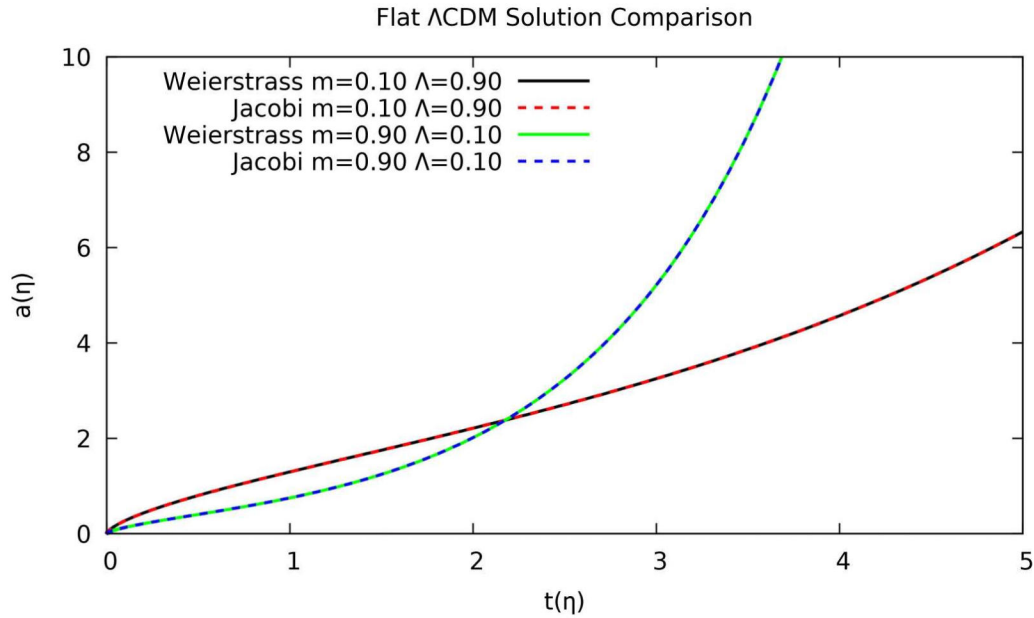


Figure 4.2: The hyperelliptic solution *Jacobi* versus the Lemaître solution *Weierstrass*.

Figure 4.2 suggests that the hyperelliptic integral method certainly works for obtaining cosmic time. This method could be a huge asset for problems where you would like to work with standard integrals and functions with intuitive properties.

## 4.4 Generalised Model Solution

It would be excellent to generalise  $\tilde{t}(\tilde{\eta})$  to include radiation and spatial curvature. We can follow the technique used to get equation (4.12) for this general model. Using equation (3.48) in the integral (4.9) we have

$$\tilde{t}(\tilde{\eta}) = \int_0^{\tilde{\eta}} \frac{\frac{1}{2}\Omega_{m,o}[\wp(\tilde{\eta}) - \frac{1}{12}\Omega_{c,o}] - \sqrt{\Omega_{r,o}\wp'(\tilde{\eta})}}{2[\wp(\tilde{\eta}) - \frac{1}{12}\Omega_{c,o}]^2 - \frac{1}{2}\Omega_{r,o}\Omega_{\Lambda}} d\tilde{\eta}'. \quad (4.39)$$

This can be split up into two integrals such that

$$\tilde{t}(\tilde{\eta}) = I_1 + I_2, \quad (4.40)$$

where

$$I_1 = \frac{\Omega_{m,o}}{4} \int_0^{\tilde{\eta}} \frac{[\wp(\tilde{\eta}) - \frac{1}{12}\Omega_{c,o}]}{[\wp(\tilde{\eta}) - \frac{1}{12}\Omega_{c,o}]^2 - \frac{1}{4}\Omega_{r,o}\Omega_\Lambda} d\tilde{\eta}', \quad (4.41)$$

and

$$I_2 = -\frac{\sqrt{\Omega_{r,o}}}{2} \int_0^{\tilde{\eta}} \frac{\wp'(\tilde{\eta})}{[\wp(\tilde{\eta}) - \frac{1}{12}\Omega_{c,o}]^2 - \frac{1}{4}\Omega_{r,o}\Omega_\Lambda} d\tilde{\eta}'. \quad (4.42)$$

The denominator can be factored

$$\left[\wp(\tilde{\eta}) - \frac{1}{12}\Omega_{c,o}\right]^2 - \frac{1}{4}\Omega_{r,o}\Omega_\Lambda = (\wp(\tilde{\eta}) - \alpha)(\wp(\tilde{\eta}) - \beta), \quad (4.43)$$

where

$$\begin{aligned} \alpha &= \frac{1}{12}\Omega_{c,o} + \frac{1}{2}\sqrt{\Omega_{r,o}\Omega_\Lambda} \\ \beta &= \frac{1}{12}\Omega_{c,o} - \frac{1}{2}\sqrt{\Omega_{r,o}\Omega_\Lambda}. \end{aligned} \quad (4.44)$$

The integrals (4.41) and (4.42) can now be split up via partial fraction decomposition

$$I_1 = \frac{\Omega_{m,o}}{8} \int_0^{\tilde{\eta}} \frac{1}{\wp(\tilde{\eta}) - \alpha} d\tilde{\eta}' + \frac{\Omega_{m,o}}{8} \int_0^{\tilde{\eta}} \frac{1}{\wp(\tilde{\eta}) - \beta} d\tilde{\eta}', \quad (4.45)$$

and

$$I_2 = \frac{-1}{2\sqrt{\Omega_\Lambda}} \int_0^{\tilde{\eta}} \frac{\wp'(\tilde{\eta})}{\wp(\tilde{\eta}) - \alpha} d\tilde{\eta}' + \frac{\Omega_{m,o}}{8} \int_0^{\tilde{\eta}} \frac{\wp'(\tilde{\eta})}{\wp(\tilde{\eta}) - \beta} d\tilde{\eta}'. \quad (4.46)$$

The integrals for  $I_2$  are simply logarithmic, and are handled easily. The integrals for  $I_1$  have the same form as (4.11), so we get a similar result. We combine the results

$$\begin{aligned} \tilde{t}(\tilde{\eta}) &= \frac{-1}{2\sqrt{\Omega_\Lambda}} \ln \left| \frac{\wp(\tilde{\eta}) - \alpha}{\wp(\tilde{\eta}) - \beta} \right| \\ &+ \frac{\Omega_m}{8} \sum_j \frac{1}{\wp'(r_j)} \left\{ \ln \left| \frac{\sigma(\tilde{\eta} - r_j)}{\sigma(\tilde{\eta} + r_j)} \right| + 2\tilde{\eta}\zeta(r_j) \right\}, \end{aligned} \quad (4.47)$$

where

$$j = \{\alpha, \beta\}, \quad r_j \in \{x | \wp(x) - j = 0\}. \quad (4.48)$$

Equation (4.47) has realised a parametric solution for any Friedmann universe with dark energy, matter, radiation, and spatial curvature. It's clear that for the case where radiation vanishes, equation (4.47) turns back into equation (4.12). What's

not clear is how the disposition of the roots in (4.48) impact the overall behaviour of the solution. We first want to know the number of solutions to an equation of the form

$$f(z) = c, \quad (4.49)$$

where  $f(z)$  is an elliptic function and  $c$  is an arbitrary complex constant. This is simply determined by the order of the function, which in our case is two [33]. These solutions are repeated modulo  $2\omega_1, 2\omega_2$  from one unit cell to another. Where a unit cell is just the fundamental period rectangle, or some translate of it. This follows from the double periodicity of elliptic functions.

A great check would be to add a small amount of radiation to the model provided by Planck. This correction is realistic since we know there should be a small amount of radiation in the universe today. At radiation matter equality we have

$$\Omega_{m,o} \frac{a_o^3}{a_{eq}^3} = \Omega_{r,o} \frac{a_o^4}{a_{eq}^4} \quad (4.50)$$

from equating the energy densities [25]. Thus we can rearrange to get

$$\Omega_{r,o} = \Omega_{m,o} \frac{a_{eq}}{a_o}. \quad (4.51)$$

We can substitute the ratio of scale factors for a corresponding redshift

$$\Omega_{r,o} = \frac{\Omega_{m,o}}{1 + z_{eq}}. \quad (4.52)$$

The point of equation (4.52) is that Planck [5] has a listed value for  $z_{eq}$  that we can use. They list  $z_{eq} = 3402$ , which together with  $\Omega_{m,o} = 0.3153$ , corresponds to  $\Omega_{r,o} = 9.265 \times 10^{-5}$ . Including the radiation will lead to a slight positive spatial curvature of  $\Omega_{c,o} = -9.265 \times 10^{-5}$ . We plot the analytical values against numerical calculation for scale factor versus proper time. The Hubble constant, matter density, and dark energy density are the same as in figure 4.1.

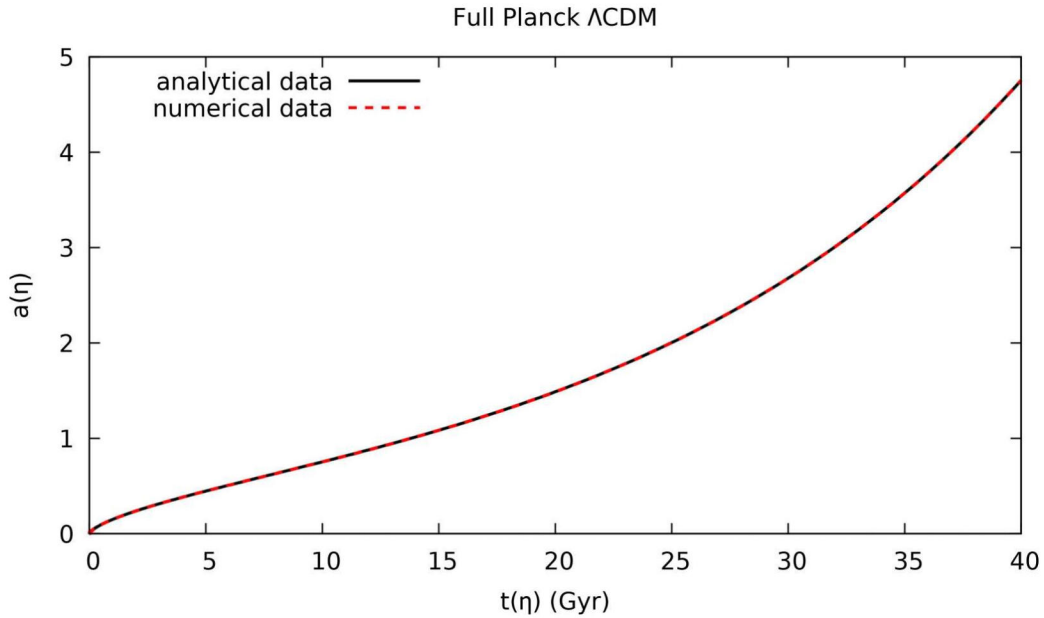


Figure 4.3: Numerical data versus analytical data for the full Planck universe.

Figure 4.3 suggests that Equation (4.47) has great agreement with numerically simulated results. The age of the universe is calculated to be 13.797 Gyr using equation (4.47). This value is in exact agreement with the data set provided by Planck [5], and the numerical data.

It's worth discussing how choices of the roots  $r_\alpha$  and  $r_\beta$  in equation (4.48) affect equation (4.47). Equation (3.52) suggests that  $r_\alpha = \tilde{\eta}_\infty$ , and indeed this is true. These values are calculated independently and found to be  $r_\alpha = \tilde{\eta}_\infty = 4.329$ . The root  $r_\beta$  on the other hand has value  $r_\beta = 4.451$ , which does not seem to be physically significant whatsoever. It's critically important also to realise that these roots are only unique modulo  $2\omega_1, 2\omega_2$  from the periodicity of  $\wp$ .

We can survey the dependence of equation (4.47) on the choice of  $r_\alpha$ , and  $r_\beta$ . Given  $g_2$ , and  $g_3$  we calculate  $e_1, e_2$ , and  $e_3$  from equation (2.21). The values of the half periods can be found using  $\wp(\omega_1) = e_1, \wp(\omega_2) = e_2$ , and  $\wp(\omega_3) = e_3$ . In the case being currently considered the periods have values  $2\omega_1 = 6.584 + 3.800i$ ,

$2\omega_2 = 6.584 - 3.800i$ , and  $2\omega_3 = 13.17$ . This set of periods forms a fundamental period parallelogram as in figure 2.3. By adding an arbitrary factor of the periods to  $r_\alpha$  and  $r_\beta$ , one can probe how equation (4.47) responds. In general this looks like

$$r'_j = r_j + 2n\omega_1 + 2m\omega_2 + 2r\omega_3 \quad n, m, r \in \mathbb{Z}, \quad (4.53)$$

where  $j = \{\alpha, \beta\}$ , and  $r'_j = r_j \bmod(2n\omega_1, 2m\omega_2)$ . Through testing with the model used for figure 4.3, we find an interesting result. Adding a shift to the roots  $r_j$  seems to have an effect on the values of  $\tilde{t}(\tilde{\eta})$ . This effect is that sometimes the shifting process adds an imaginary offset to  $\tilde{t}(\tilde{\eta})$ . The offset can be eliminated by remembering that time should only be a real number, and not complex. Therefore it's reasonable to take the real part and ignore any imaginary contribution. The occurrence of this offset makes sense intuitively because equation (4.47) depends on the  $\zeta$  and  $\sigma$  functions which are only quasi periodic. Why the offset is purely imaginary is unknown, but at least a nice coincidence. We insist that this evidence is purely exploratory, and that a mathematical proof would be necessary for general conclusions. It's reasonable to ignore complex roots where possible, since our ideal range of  $\tilde{\eta}$  is purely real anyways. Though there may be toy universe models where it is not possible to avoid a complex set of roots  $r_j$ .

Consider a model where  $\Omega_\Lambda = 0.1$ ,  $\Omega_{m,o} = 2.6$ ,  $\Omega_{r,o} = 0.5$ , and  $\Omega_{c,o} = -2.2$ . This example is chosen to highlight the case where the universe is cyclic, and therefore certainly has no limiting conformal time  $\eta_\infty$ . We can verify this by plotting the scale factor versus the cosmic proper time.

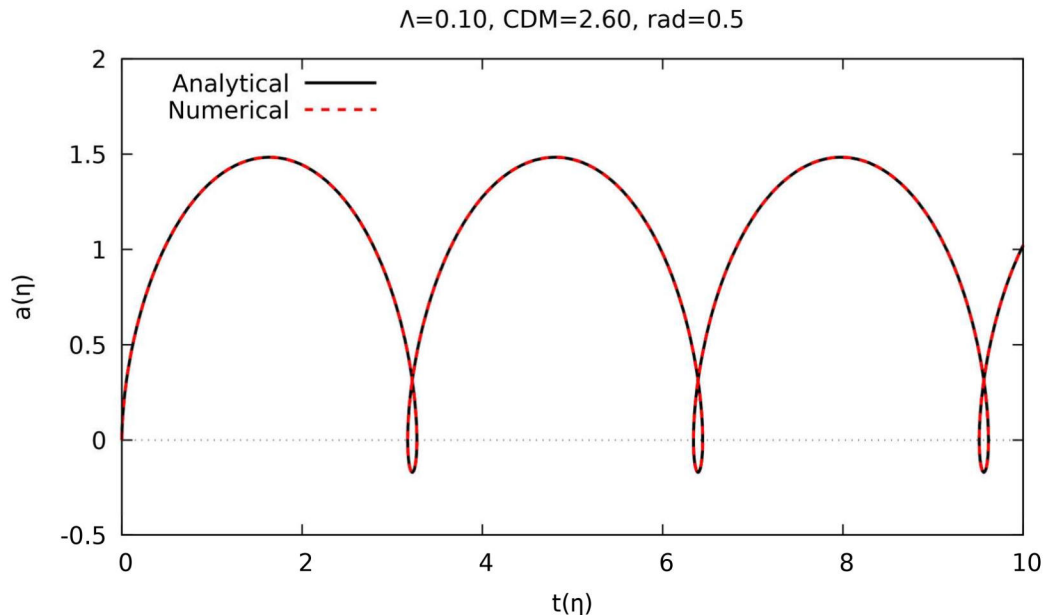


Figure 4.4: Numerical data versus analytical data for a collapsing universe with matter, dark energy, curvature, and radiation.

Figure 4.4 has a number of features that stand out. The parameterized solution takes the form of a prolate cycloid, and hence has some very nonphysical behaviour. Having the cosmos become negative in size while travelling backwards in cosmic proper time is not going to be physically realizable. The periods of  $\varphi$  in this case are  $2\omega_1 = 4.647$ ,  $2\omega_2 = 4.415i$ , and  $2\omega_3 = 4.467 + 4.415i$ . This set of periods forms a fundamental period parallelogram as in figure 2.2. The roots  $r_j$  needed for  $t(\eta)$  are complex this time. They take on the values  $r_\alpha = 3.252 + 2.207i$ , and  $r_\beta = 4.168 + 2.207i$  modulo the periods. Once again there is an imaginary offset for the values of cosmic time, but we simply take the real part.

Equation (4.47) has very successfully been used in figures 4.3 and 4.4. The logarithmic parts of  $t(\eta)$  have the absolute value taken to reduce any headache caused by imaginary values. In order to eliminate the headache entirely, it's reasonable to

rewrite equation (4.47) as

$$\tilde{t}(\tilde{\eta}) = \frac{-1}{2\sqrt{\Omega_\Lambda}} \ln \left| \frac{\wp(\tilde{\eta}) - \alpha}{\wp(\tilde{\eta}) - \beta} \right| + \frac{\Omega_m}{8} \sum_j \frac{1}{\wp'(r_j)} \ln \left| \frac{\sigma(\tilde{\eta} - r_j)}{\sigma(\tilde{\eta} + r_j)} e^{2\tilde{\eta}\Re[\zeta(r_j)]} \right|. \quad (4.54)$$

The idea behind equation (4.54) is that now there is no imaginary offset in  $t(\eta)$ , given any choice of  $r_j$ . This is not a necessary change, but it does make calculation a little more concise.

## 4.5 Redshift Drift

When the scale factor of the universe increases, the way it continues to change changes. This fact is very clear from the strong nonlinearity of the Friedmann equation. Since the cosmic scale factor is what defines the cosmic redshift, a drift in this redshift may therefore be detected. Consider a light signal emitted at conformal time  $\eta_{em}$  from a galaxy at conformal distance  $\chi$  away. The signal is observed at conformal time  $\eta_{ob}$  so

$$\eta_{ob} - \chi = \eta_{em}, \quad (4.55)$$

and thus

$$d\eta_{ob} = d\eta_{em}. \quad (4.56)$$

The cosmic redshift is found via equation (3.9)

$$1 + z = \frac{a(t_{ob})}{a(t_{em})} = \frac{dt_{ob}}{dt_{em}}. \quad (4.57)$$

Switching to conformal time we have

$$\frac{dt_{ob}}{dt_{em}} = \frac{a(\eta_{ob})d\eta_{ob}}{a(\eta_{em})d\eta_{em}}, \quad (4.58)$$

and now

$$1 + z = \frac{a(t_{ob})}{a(t_{em})} = \frac{a(\eta_{ob})}{a(\eta_{ob} - \chi)}. \quad (4.59)$$

**Redshift drift** is taken to mean

$$\frac{dz}{dt_{ob}} = \dot{z} = \frac{\dot{a}(t_{ob})}{a(t_{em})} - \frac{a(t_{ob})}{a(t_{em})} \frac{\dot{a}(t_{em})}{a(t_{em})}. \quad (4.60)$$

In terms of conformal time this becomes

$$\dot{z} = \frac{\dot{a}(\eta)}{a(\eta - \chi)} - \frac{a(\eta)}{a(\eta - \chi)} \frac{\dot{a}(\eta - \chi)}{a(\eta - \chi)}. \quad (4.61)$$

Recognizing that from the chain rule of calculus

$$\frac{da(\eta)}{dt_{ob}} = \frac{da(\eta)}{d\eta} \frac{d\eta}{dt_{ob}} = \frac{a'(\eta)}{a(\eta)}, \quad (4.62)$$

equation (4.61) becomes

$$\dot{z} = \frac{a'(\eta)}{a(\eta)a(\eta - \chi)} - \frac{a'(\eta - \chi)}{[a(\eta - \chi)]^2}. \quad (4.63)$$

We can use dimensionless quantities

$$\tilde{z} = \frac{\tilde{a}'(\tilde{\eta})}{\tilde{a}(\tilde{\eta})\tilde{a}(\tilde{\eta} - \tilde{\chi})} - \frac{\tilde{a}'(\tilde{\eta} - \tilde{\chi})}{[\tilde{a}(\tilde{\eta} - \tilde{\chi})]^2}. \quad (4.64)$$

Defining a conformal Hubble parameter

$$\tilde{\mathcal{H}}(\tilde{\eta}) \stackrel{\text{def}}{=} \frac{\tilde{a}'(\tilde{\eta})}{\tilde{a}(\tilde{\eta})}, \quad (4.65)$$

we write equation (4.64) as

$$\tilde{z} = \frac{\tilde{\mathcal{H}}(\tilde{\eta}) - \tilde{\mathcal{H}}(\tilde{\eta} - \tilde{\chi})}{\tilde{a}(\tilde{\eta} - \tilde{\chi})}. \quad (4.66)$$

Equation (4.66) gives us information for the redshift drift as a function of the observer's conformal time  $\tilde{\eta}$  and the conformal distance  $\tilde{\chi}$ . It's common to take the observer's time as time now, and then equation (4.60) becomes

$$\dot{z} = (1 + z)H_o - H(z), \quad (4.67)$$

where

$$H(z) = H_o \left[ \sum_i \Omega_{i,o} (1 + z)^{3(1+w_i)} \right]^{\frac{1}{2}} \quad (4.68)$$

is just the Friedmann equation in terms of redshift. This simplification is of interest to the experimental community [13, 17]. This is because the redshift drift of an object will not change much over the course of even a century. Therefore matching

astronomical data to equation (4.67) would allow for a *model-independent* verification for the  $\Lambda$ CDM model. This is extremely important because our current understanding of the cosmos depends on the modelling of other physics, and so those models must be exactly correct for our cosmological model to be without error. The original evidence for an accelerating expansion of the universe [26] depends on our understanding of supernovae. The data used in this thesis for modelling “our cosmos” [5] depends on our understanding of the cosmic microwave background. The resulting values for the cosmological parameters from these two methodologies are not consistent. Therefore a model independent avenue for obtaining data is of such great significance.

Equation (4.66) is still of interest however. We do not measure scale factor directly, but instead redshift. Therefore any dynamical information involving redshift is significant. Furthermore, we can also verify easily that equation (4.67) is a suitable approximation for astronomical surveys. Consider comparing the redshift drift of many objects at two different times. Select one time to be time now and the other time to be after a time period “big to us but small to the universe” such as 100 years. The dimensionless redshift drift is approximately

$$\tilde{z}(\tilde{\chi}) \approx \frac{z(\tilde{\eta}_{100}, \tilde{\chi}) - z(\tilde{\eta}_o, \tilde{\chi})}{100H_o}. \quad (4.69)$$

We can compare the exact equation (4.66) with the approximate equation (4.69) by plotting redshift drift versus redshift.

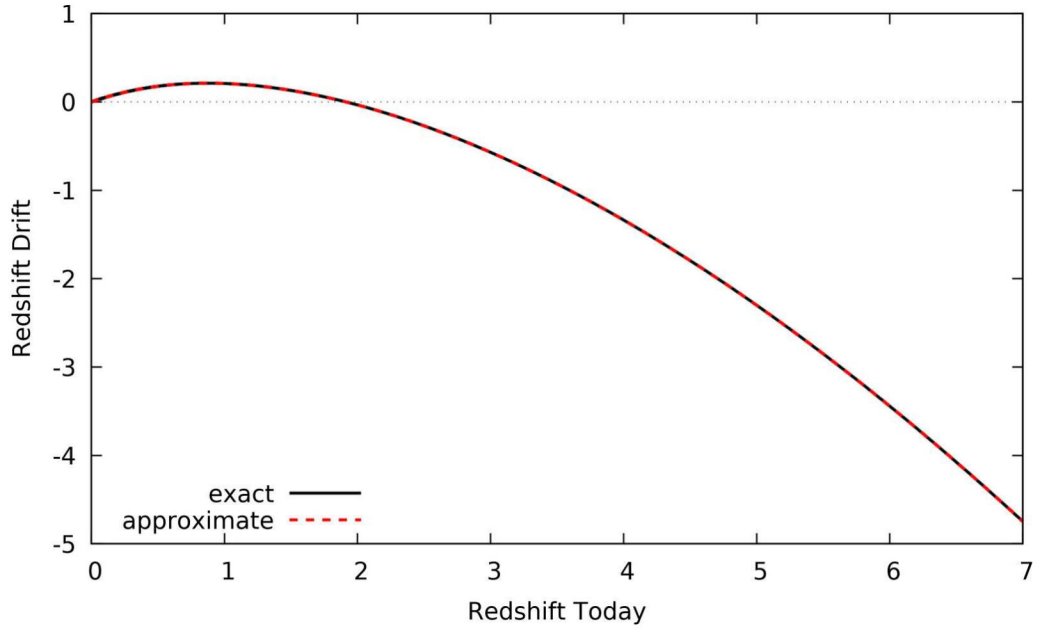


Figure 4.5: Comparison of exact redshift drift and a realistic approximation.

The difference in the value of redshift drifts over the 100 year period is

$$\Delta\tilde{z} = \tilde{z}(\tilde{\chi}, \tilde{\eta}_{100}) - \tilde{z}(\tilde{\chi}, \tilde{\eta}_0). \quad (4.70)$$

Figure 4.5 is the well-known graph that is often plotted by equation (4.67). Liske et al. have a similar plot with slightly different universes [13]. Equation (4.70) may be plotted to show the magnitude of change in the redshift drift over the 100 year interval.

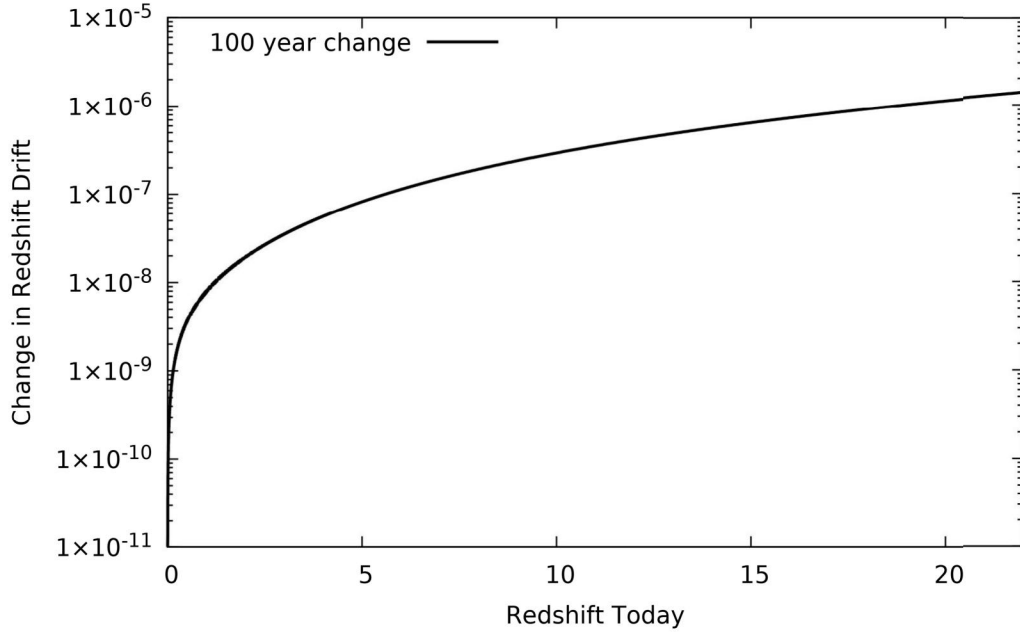


Figure 4.6: The order of magnitude for the change in redshift drifts over 100 years.

The parameters used for figures 4.5 and 4.6 are once again the Planck collaboration 2018 data. It's of no surprise that over a 100 year period of time the redshift drift for any object we could detect would not measurably change. This gives astronomers a lot of leeway in measuring redshift drift. This measurement would be important because we would gain a model independent verification of the  $\Lambda$ CDM model via equation (4.67). Take for example an object at a redshift at time now of  $z_o = 7.27$ . Using our exact expressions for cosmic time, redshift, and redshift drift we can track the evolution of the detected signal over time.

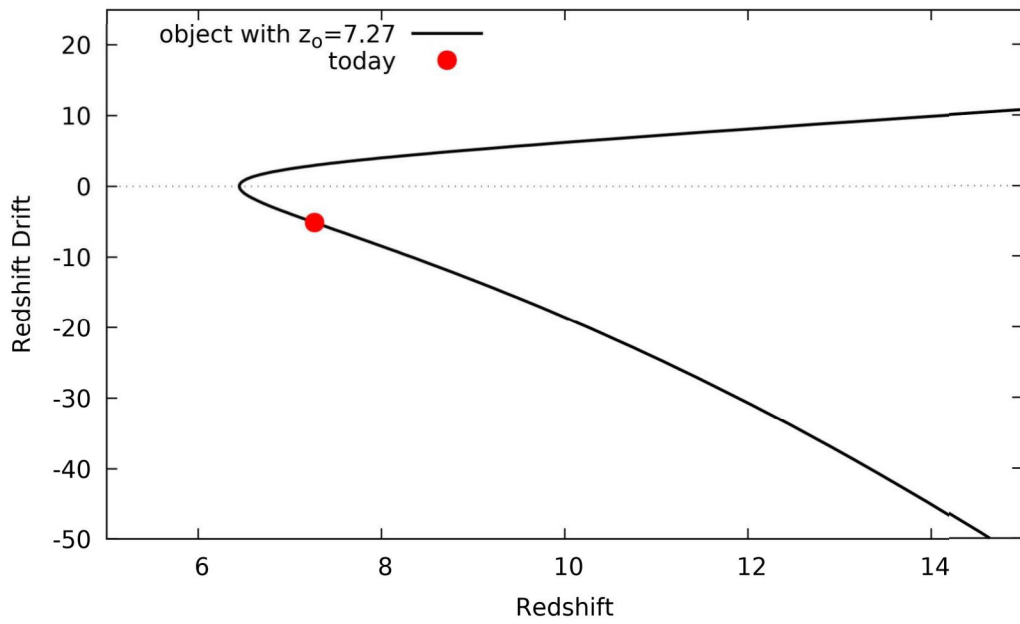


Figure 4.7: Redshift drift versus redshift for an object in our universe. Redshift drift is increasing with cosmic time for all times, but redshift may be increasing or decreasing with cosmic time for some times.

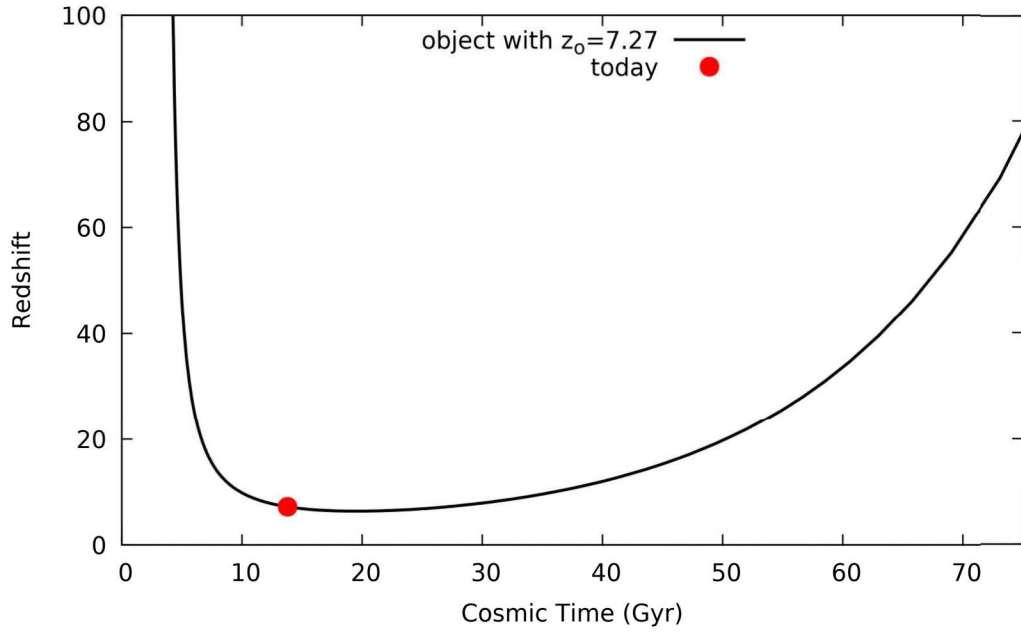


Figure 4.8: Redshift versus cosmic time of an object in our universe.

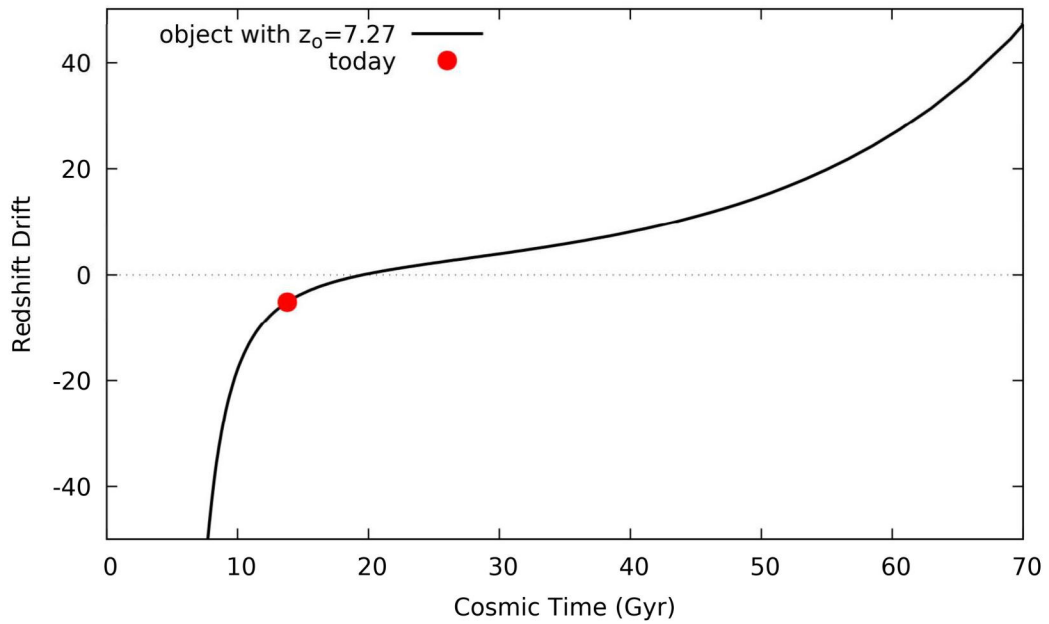


Figure 4.9: Redshift drift versus cosmic time of an object in our universe.

The importance of figures 4.7, 4.8, and 4.9 is largely related to our perception of signals from distant objects in the universe. At time now there may be objects that have either increasing or decreasing redshift relative to us. This is a direct result of the high nonlinearity of the Friedmann equation. Every object with distinct redshift today conveys a unique depiction of the expansion history of the universe. Thus detecting signals from many redshifts is necessary to understand the nonlinear expansion completely.

This section has demonstrated that an exact solution to the standard  $\Lambda$ CDM model is useful for plotting a wide range of dynamic quantities. In figures 4.7, 4.8, and 4.9, equation (4.54) was used to calculate cosmic times, and scale factors were calculated using equation (3.48). These expressions have provided data that compares well with numerical analysis and plots provided by literature.

## 4.6 Limiting Cases

A popular theme in physics is to see whether or not a more complicated model can be approximated down to a more simple one. A famous example is deriving Newton's law of gravitation through the formalism of general relativity. This section highlights agreement between equations (4.54) and (3.48) versus other more simple known expressions. For convenience I copy down the general Friedmann model equations

$$\tilde{a}(\tilde{\eta}) = \frac{\frac{1}{2}\Omega_{m,o}[\wp(\tilde{\eta}) - \frac{1}{12}\Omega_{c,o}] - \sqrt{\Omega_{r,o}}\wp'(\tilde{\eta})}{2[\wp(\tilde{\eta}) - \frac{1}{12}\Omega_{c,o}]^2 - \frac{1}{2}\Omega_{r,o}\Omega_{\Lambda}}, \quad (4.71)$$

where

$$\wp(\tilde{\eta}) \stackrel{\text{def}}{=} \wp(\tilde{\eta}|g_2, g_3), \quad (4.72)$$

with

$$g_2 = \Omega_{\Lambda}\Omega_{r,o} + \frac{1}{12}\Omega_{c,o}^2, \quad g_3 = \frac{1}{6}\Omega_{\Lambda}\Omega_{r,o}\Omega_{c,o} - \frac{1}{16}\Omega_{\Lambda}\Omega_{m,o}^2 - \frac{1}{216}\Omega_{c,o}^3. \quad (4.73)$$

$$\begin{aligned} \tilde{t}(\tilde{\eta}) &= \frac{-1}{2\sqrt{\Omega_\Lambda}} \ln \left| \frac{\wp(\tilde{\eta}) - \alpha}{\wp(\tilde{\eta}) - \beta} \right| \\ &+ \frac{\Omega_m}{8} \sum_j \frac{1}{\wp'(r_j)} \left\{ \ln \left| \frac{\sigma(\tilde{\eta} - r_j)}{\sigma(\tilde{\eta} + r_j)} \right| + 2\tilde{\eta}\zeta(r_j) \right\}, \end{aligned} \quad (4.74)$$

where

$$j = \{\alpha, \beta\}, \quad r_j \in \{x | \wp(x) - j = 0\}, \quad (4.75)$$

and

$$\begin{aligned} \alpha &= \frac{1}{12}\Omega_{c,o} + \frac{1}{2}\sqrt{\Omega_{r,o}\Omega_\Lambda} \\ \beta &= \frac{1}{12}\Omega_{c,o} - \frac{1}{2}\sqrt{\Omega_{r,o}\Omega_\Lambda}. \end{aligned} \quad (4.76)$$

#### 4.6.1 Dark Energy and Matter

If radiation and curvature are discarded then  $g_2 = 0$ ,  $g_3 = -\frac{1}{16}\Omega_\Lambda\Omega_{m,o}^2$ ,  $\alpha = \beta = 0$ , and  $r_j \in \{x | \wp(x) = 0\}$ , so we can say  $r_j = \tilde{\eta}_\infty$ . Thus the model is exactly what was discussed in section 4.2.

#### 4.6.2 Dark Energy, Matter, and Spatial Curvature

If radiation is discarded then the scale factor becomes

$$\tilde{a}(\tilde{\eta}) = \frac{\Omega_{m,o}}{4[\wp(\tilde{\eta}) - \frac{1}{12}\Omega_{c,o}]}, \quad (4.77)$$

where

$$\wp(\tilde{\eta}) \stackrel{\text{def}}{=} \wp(\tilde{\eta}; g_2, g_3), \quad (4.78)$$

with

$$g_2 = \frac{1}{12}\Omega_{c,o}^2, \quad g_3 = -\frac{1}{16}\Omega_\Lambda\Omega_{m,o}^2 - \frac{1}{216}\Omega_{c,o}^3. \quad (4.79)$$

The cosmic time is now

$$\tilde{t}(\tilde{\eta}) = \frac{\Omega_m}{8} \sum_j \frac{1}{\wp'(r_j)} \left\{ \ln \left| \frac{\sigma(\tilde{\eta} - r_j)}{\sigma(\tilde{\eta} + r_j)} \right| + 2\tilde{\eta}\zeta(r_j) \right\}, \quad (4.80)$$

where

$$j = \{\alpha, \beta\}, \quad r_j \in \{x | \wp(x) - j = 0\}, \quad (4.81)$$

and

$$\alpha = \beta = \frac{1}{12}\Omega_{c,o}. \quad (4.82)$$

Note that  $r_j$  is not just  $\tilde{\eta}_\infty$  because it's possible that the universe is cyclic. It was shown in section 4.4 that you do not have a limiting conformal time provided enough positive spatial curvature. Instead we denote this potentially complex root as  $\tilde{\eta}_x$ .

$$\tilde{t}(\tilde{\eta}) = \frac{\Omega_m}{4} \frac{1}{\wp'(\tilde{\eta}_x)} \left\{ \ln \left| \frac{\sigma(\tilde{\eta} - \tilde{\eta}_x)}{\sigma(\tilde{\eta} + \tilde{\eta}_x)} \right| + 2\tilde{\eta}\zeta(\tilde{\eta}_x) \right\} \quad (4.83)$$

This model is derived by Lemaître [22].

### 4.6.3 Matter, Spatial Curvature, and Radiation

Elliptic functions are not needed in any case without dark energy. The scale factor can still be found from equation (4.71) using some identities. The cosmic time is then just the integral of that result; equation (4.74) will clearly not tolerate vanishing dark energy. There are three sub cases because the spatial curvature term may be open, flat, or closed. We start with the scale factor for all three cases

$$\tilde{a}(\tilde{\eta}) = \frac{\frac{1}{2}\Omega_{m,o}[\wp(\tilde{\eta}) - \frac{1}{12}\Omega_{c,o}] - \sqrt{\Omega_{r,o}}\wp'(\tilde{\eta})}{2[\wp(\tilde{\eta}) - \frac{1}{12}\Omega_{c,o}]^2}, \quad (4.84)$$

where

$$\wp(\tilde{\eta}) \stackrel{\text{def}}{=} \wp(\tilde{\eta}; g_2, g_3), \quad (4.85)$$

with

$$g_2 = \frac{1}{12}\Omega_{c,o}^2, \quad g_3 = -\frac{1}{216}\Omega_{c,o}^3. \quad (4.86)$$

The modular invariants are special in this case and identities from [1] lead to

$$\wp(\tilde{\eta}) = \begin{cases} \frac{|\Omega_{c,o}|}{12} + \frac{|\Omega_{c,o}|}{4} \left[ \sinh \left( \sqrt{\frac{|\Omega_{c,o}|}{12}} \tilde{\eta} \right) \right]^{-2} & \Omega_{c,o} > 0 \\ \tilde{\eta}^{-2} & \Omega_{c,o} = 0 \\ -\frac{|\Omega_{c,o}|}{12} + \frac{|\Omega_{c,o}|}{4} \left[ \sin \left( \sqrt{\frac{|\Omega_{c,o}|}{12}} \tilde{\eta} \right) \right]^{-2} & \Omega_{c,o} < 0. \end{cases} \quad (4.87)$$

The scale factor in each case is

$$\tilde{a}(\tilde{\eta}) = \begin{cases} \frac{\Omega_{m,o}}{|\Omega_{c,o}|} \sinh^2 \left( \frac{\sqrt{|\Omega_{c,o}|}}{2} \tilde{\eta} \right) + \frac{2\sqrt{\Omega_{r,o}}}{\sqrt{|\Omega_{c,o}|}} \cosh \left( \frac{\sqrt{|\Omega_{c,o}|}}{2} \tilde{\eta} \right) \sinh \left( \frac{\sqrt{|\Omega_{c,o}|}}{2} \tilde{\eta} \right) & \Omega_{c,o} > 0 \\ \frac{\Omega_{m,o}}{4} \tilde{\eta}^2 + \sqrt{\Omega_{r,o}} \tilde{\eta} & \Omega_{c,o} = 0 \\ \frac{\Omega_{m,o}}{|\Omega_{c,o}|} \sin^2 \left( \frac{\sqrt{|\Omega_{c,o}|}}{2} \tilde{\eta} \right) + \frac{2\sqrt{\Omega_{r,o}}}{\sqrt{|\Omega_{c,o}|}} \cos \left( \frac{\sqrt{|\Omega_{c,o}|}}{2} \tilde{\eta} \right) \sin \left( \frac{\sqrt{|\Omega_{c,o}|}}{2} \tilde{\eta} \right) & \Omega_{c,o} < 0. \end{cases} \quad (4.88)$$

Integrating the scale factor provides the cosmic time

$$\tilde{t}(\tilde{\eta}) = \begin{cases} \frac{\Omega_{m,o}}{2\sqrt{|\Omega_{c,o}|^3}} \left[ \sinh \left( \sqrt{|\Omega_{c,o}|} \tilde{\eta} \right) - \sqrt{|\Omega_{c,o}|} \tilde{\eta} \right] + \frac{2\sqrt{\Omega_{r,o}}}{|\Omega_{c,o}|} \sinh^2 \left( \frac{\sqrt{|\Omega_{c,o}|}}{2} \tilde{\eta} \right) & \Omega_{c,o} > 0 \\ \frac{\Omega_{m,o}}{12} \tilde{\eta}^3 + \frac{\sqrt{\Omega_{r,o}}}{2} \tilde{\eta}^2 & \Omega_{c,o} = 0 \\ \frac{-\Omega_{m,o}}{2\sqrt{|\Omega_{c,o}|^3}} \left[ \sin \left( \sqrt{|\Omega_{c,o}|} \tilde{\eta} \right) - \sqrt{|\Omega_{c,o}|} \tilde{\eta} \right] + \frac{2\sqrt{\Omega_{r,o}}}{|\Omega_{c,o}|} \sin^2 \left( \frac{\sqrt{|\Omega_{c,o}|}}{2} \tilde{\eta} \right) & \Omega_{c,o} < 0. \end{cases} \quad (4.89)$$

The positively curved case may be used to highlight one of the important features of dark energy. You may have dark energy in a model without the model expanding forever. We consider the parameters used in figure 4.4 but compare the analytical expressions to ones without any dark energy.

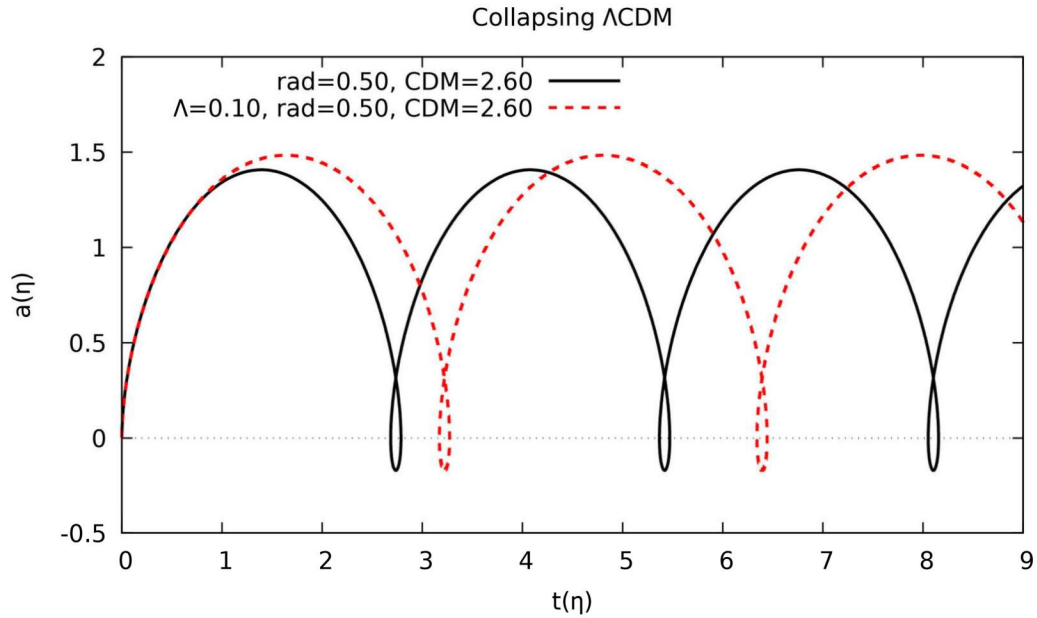


Figure 4.10: The “stalling” or “loitering” effect of dark energy highlighted with a cyclic universe.

Figure 4.10 clearly highlights that dark energy is sometimes not strong enough to overcome strong positive spatial curvature. Equations (3.87) and (3.88) can be found in Ellis et al [12]. If radiation is excluded there is a nice expression for the amount of dark energy required to stop a universe from collapsing. Carroll [3] provides

$$\Omega_{\Lambda} \geq \begin{cases} 0, & 0 \leq \Omega_{m,o} \leq 1 \\ 4\Omega_{m,o} \cos^3 \left[ \frac{1}{3} \cos^{-1} \left( \frac{1-\Omega_{m,o}}{\Omega_{m,o}} \right) + \frac{4\pi}{3} \right], & \Omega_{m,o} > 1. \end{cases} \quad (4.90)$$

Equation (4.90) is a nice to have when looking at the matter, curvature, and dark energy model discussed in section 3.6.2. Another special case that is useful for comparison is where we get rid of radiation and only have matter and spatial curvature.

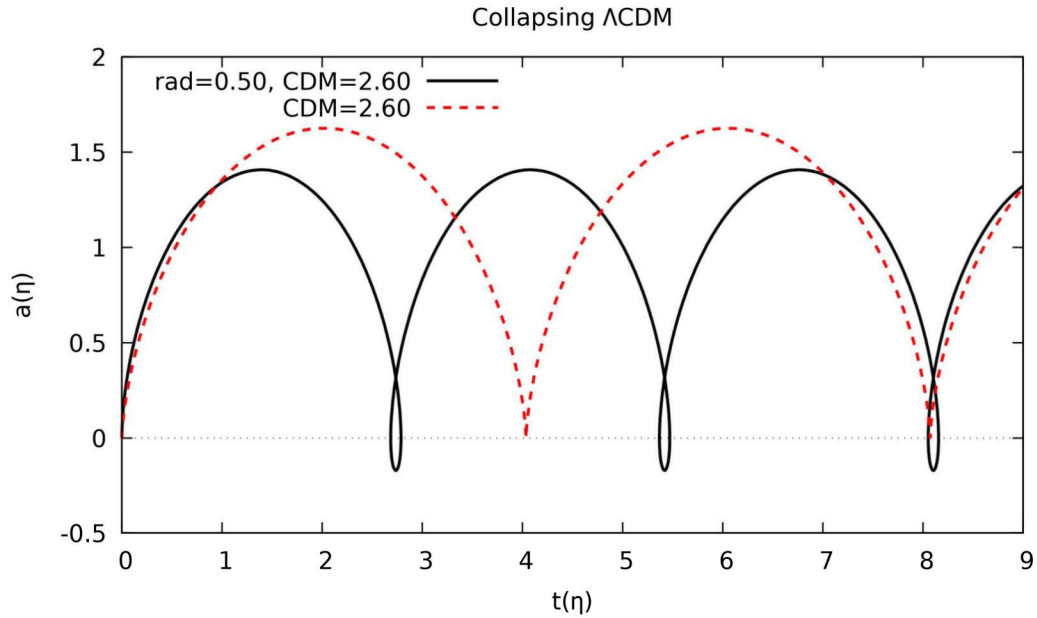


Figure 4.11: The “looping” effect of radiation compared to matter only.

Figure 4.11 highlights the effect of radiation on model with strong positive spatial curvature. Without radiation the “loops” in figure 4.10 disappear and leave us with the well studied collapsing universe without radiation or dark energy. Clearly the parametric solution for the Friedmann equation does not always uniquely determine the scale factor at all cosmic times. Indeed one has to use physical reasoning to discard bad mathematical components of a model. For example you would probably interpret figure 4.10 as having models where after some “big bang” at time zero the universes expands to some maximum, and then subsequently there is a “big crunch” later at some other time. The other information is most likely entirely unphysical because the FLRW metric is not valid in the limit as the scale factor becomes zero. That is to say we do not have information about the cosmos at these critical points. It would be interesting to have a cyclic universe, or even one where the size becomes negative as cosmic time flows backwards. One could also argue that these collapsing models are unphysical because our own universe does not seem to entertain such

parameters.

Other special cases become quite simple, and are found in cosmology texts such as Ryden [28]. The following chapter summarizes and concludes the results obtained in this thesis.

# Chapter 5

## Conclusion

Elliptic functions have been used to model problems in physics for at least over a century. Many systems that exhibit strong nonlinearities have elliptic function solutions. It has been known for a long time that the Friedmann equation including cosmological constant admits this type of behaviour. What was not known was how other quantities including cosmic time could be calculated from these expressions. This thesis has provided insight into this question. An exact parametric solution to the Friedmann equation including matter, spatial curvature, radiation, and dark energy was presented. This solution was then used to calculate other important dynamical quantities for the cosmos as we understand it today. The elliptic function technique has been shown to be a powerful tool for mathematical physicists.

It's absolutely worth discussing how the change in computer technology has impacted special function research. Tables of special function values were your only hope before computer algebra systems became widely available. This would have artificially limited your parameter space to one where you have a set of given values. One can calculate much more with modern programs such as Maple. This has made special functions much more reliable in the same way that numerical analysis is now much easier to do. The combination of both special function techniques and numerical analysis allows researchers to be very confident when solving difficult nonlinear

systems. Relying on a single technique to provide raw data is never optimal and can sometimes cause erroneous results to be published. In sections 4.3 and 4.4 I found that the parameter space of the standard Friedmann universe was fairly complicated. If solutions had simply been written down and not actually used it would have been extremely easy to miss this idea. Part of the hyperelliptic solution would have been wrong for the spatially flat universe discussed in section 4.3. Analysis of the roots required for the general solution of cosmic time in terms of Weierstrass functions may have been unclear. Modern computing systems are integral for understanding complex nonlinear system like the standard  $\Lambda$ CDM model of cosmology.

Whether or not our standard model of cosmology is really the correct description of the universe on a large scale is still a hot topic of debate. Additions to the model have been postulated in recent years to try and remedy certain issues with intergalactic observations. Though it's probably not worth considering an addition to the model unless a large break in isotropy or homogeneity is ever detected. A more complicated spacetime metric would need to be used in the case that either assumption is broken. The equations considered in this thesis say nothing about the universe on smaller scales, and instead seek to shed light on only the most expansive scales. Therefore it's not worth considering the addition of other physics to the model except in the context of a toy theory.

It remains to be seen whether redshift drift will echo the predictions of the standard  $\Lambda$ CDM model. Verifying and honing this model to higher precision is of great interest to the cosmology community. Having a set of data for redshift drift at many redshifts could verify the validity of the model. If figure 4.5 can not be created then there would clearly be a huge problem with the standard model of cosmology. Though this would rather surprising in contrast to the CMB data, and many other data sets.

The data used to create the current accurate "Planck" model in this thesis was not coincidentally selected. It's not that it was considered the most physically significant, but instead it avoids discussion of difficult experimental astrophysics. Analysing the

CMB fits intuitively very well with discussions of the universe on the largest scales. Other astrophysical data may involve discussing ideas such as standard candles and various stellar objects. The Planck 2018 data is also simply some of the newest data available, and is widely cited.

Limiting cases were discussed in some detail in section 4.6. The cases provided were selected to highlight the similarities and differences between models with and without dark energy. The dark energy term in the Friedmann equation is what leads to the elliptic function solution after all. Dark energy appears to play two general roles in cosmic dynamics. If dark energy is dominant, then a model will eventually experience an accelerated expansion. If dark energy is not dominant with large positive spatial curvature, then instead it can cause the scale factor to “stall” or “loiter” before the universe subsequently collapses. Figure 4.10 describes an example of the latter case, and figure 4.3 and example of the former. Comparing various Friedmann models is interesting because it sheds some light on the unique contributions of each cosmic fluid considered.

Elliptic functions continue to be used in many areas of physics. Some research has even been aimed at comparing systems described by the same equation. A paper of Faraoni [16] looks at many phenomena with properties described by the Friedmann equation. Therefore it’s reasonable to suggest that the research included in this thesis could be used in a wide range of engineering, physics, and biology applications. Perhaps future work could even explore how various systems differ in parameter space. Classifying problems based on evolutionary equations may not be a new idea, but it remains of great interest to the mathematical physics community.

# Appendix A

## Numerical Methods

### A.1 Friedmann Equation Discretization

The differential equation

$$[\tilde{a}'(\tilde{\eta})]^2 = \Omega_\Lambda [\tilde{a}(\tilde{\eta})]^4 + \Omega_{c,o} [\tilde{a}(\tilde{\eta})]^2 + \Omega_{m,o} [\tilde{a}(\tilde{\eta})] + \Omega_{r,o} \quad (\text{A.1})$$

and the integral

$$\tilde{t}(\tilde{\eta}) = \int_0^{\tilde{\eta}} \tilde{a}(\tilde{\eta}') d\tilde{\eta}' \quad (\text{A.2})$$

can be solved numerically. First raise the order of equation (A.1) by taking a derivative

$$2[\tilde{a}'(\tilde{\eta})][\tilde{a}''(\tilde{\eta})] = 4\Omega_\Lambda [\tilde{a}(\tilde{\eta})]^3 [\tilde{a}'(\tilde{\eta})] + 2\Omega_{c,o} [\tilde{a}(\tilde{\eta})][\tilde{a}'(\tilde{\eta})] + \Omega_{m,o} [\tilde{a}'(\tilde{\eta})]. \quad (\text{A.3})$$

We simplify equation (A.3)

$$[\tilde{a}''(\tilde{\eta})] = 2\Omega_\Lambda [\tilde{a}(\tilde{\eta})]^3 + \Omega_{c,o} [\tilde{a}(\tilde{\eta})] + \frac{1}{2}\Omega_{m,o}. \quad (\text{A.4})$$

Now we can lower the order of equation A.4 by turning it into a system of two first order equations. Let  $u = \tilde{a}(\tilde{\eta})$  and  $v = \tilde{a}'(\tilde{\eta})$ , then

$$u' = v, \quad v' = 2\Omega_\Lambda u^3 + \Omega_{c,o}u + \frac{1}{2}\Omega_{m,o}. \quad (\text{A.5})$$

The system of equations (A.5) can be solved via two-dimensional fourth order Runge-Kutta. The integral (A.2) can be done in tandem with the differential equation using the trapezoidal rule on each iteration. Let  $x = \tilde{\eta}$  and  $t = \tilde{t}(\tilde{\eta})$ . Now let  $u' = f(x, u, v)$  and  $v' = g(x, u, v)$  with initial values  $x_i = 0$ ,  $t_i = 0$ ,  $u_i = 0$ , and  $v_i = \sqrt{\Omega_{r,o}}$ . If  $h$  is some chosen step size then let

$$n = \frac{x - x_i}{h} \quad (\text{A.6})$$

be the number of steps where  $x$  is the chosen value of conformal time. If  $j = 1, \dots, n$  then our system solves as

$$k_1 = hf(x_j, u_j, v_j) \quad (\text{A.7})$$

$$l_1 = hg(x_j, u_j, v_j) \quad (\text{A.8})$$

$$k_2 = hf\left(x_j + \frac{1}{2}h, u_j + \frac{1}{2}k_1, v_j + \frac{1}{2}l_1\right) \quad (\text{A.9})$$

$$l_2 = hg\left(x_j + \frac{1}{2}h, u_j + \frac{1}{2}k_1, v_j + \frac{1}{2}l_1\right) \quad (\text{A.10})$$

$$k_3 = hf\left(x_j + \frac{1}{2}h, u_j + \frac{1}{2}k_2, v_j + \frac{1}{2}l_2\right) \quad (\text{A.11})$$

$$l_3 = hg\left(x_j + \frac{1}{2}h, u_j + \frac{1}{2}k_2, v_j + \frac{1}{2}l_2\right) \quad (\text{A.12})$$

$$k_4 = hf(x_j + h, u_j + k_3, v_j + l_3) \quad (\text{A.13})$$

$$l_4 = hg(x_j + h, u_j + k_3, v_j + l_3) \quad (\text{A.14})$$

$$u_{j+1} = \frac{1}{6}(k_1 + 2k_2 + 2k_3 + k_4) \quad (\text{A.15})$$

$$v_{j+1} = \frac{1}{6}(l_1 + 2l_2 + 2l_3 + l_4) \quad (\text{A.16})$$

$$x_{j+1} = x_j + h \quad (\text{A.17})$$

$$t_{j+1} = t_j + \frac{1}{2}h(u_j + u_{j+1}). \quad (\text{A.18})$$

This method is more than sufficient for basic numerical results. Absolute error calculations are done using the standard idea

$$\delta f_{absolute} = |f_{exact} - f_{numerical}|. \quad (\text{A.19})$$

For example consider the numerical and Lemaître solution data as in figure 3.1.

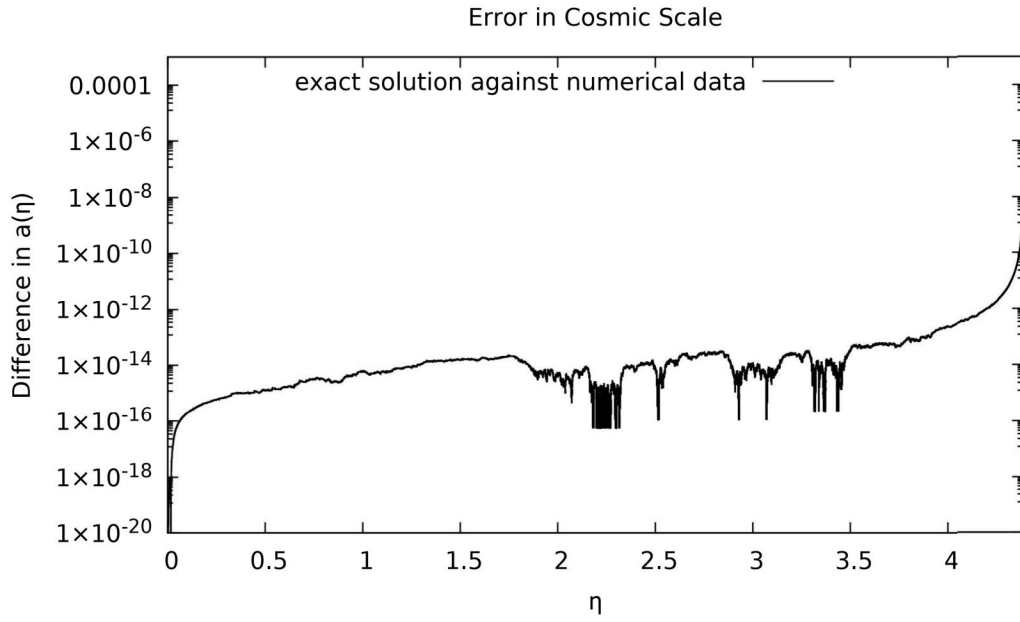


Figure A.1: The agreement between exact and numerical results for cosmic scale.

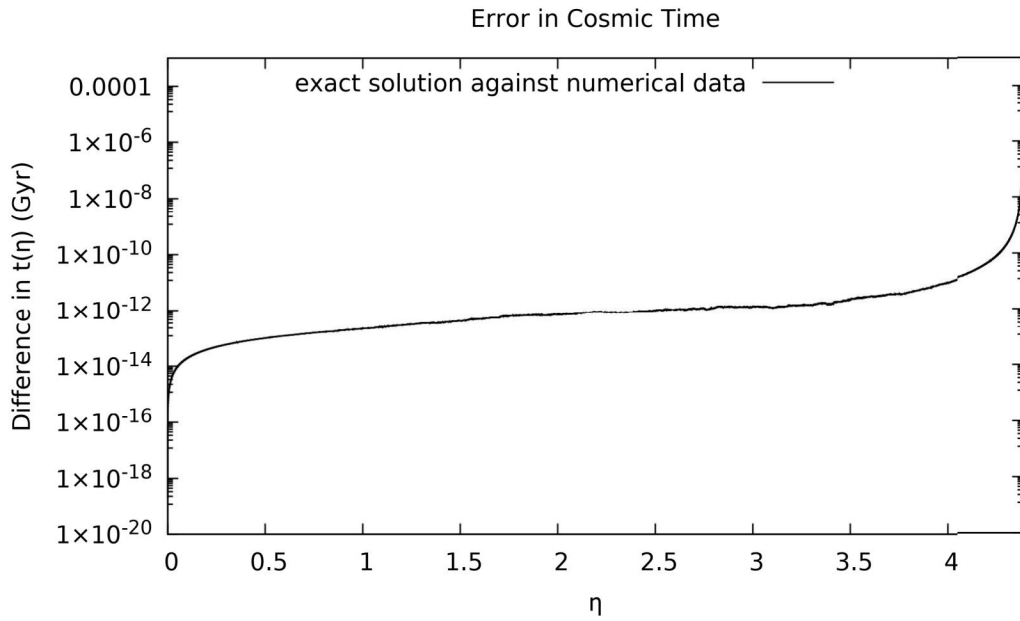


Figure A.2: The agreement between exact and numerical results for cosmic time.

The agreement between numerical and analytical results is absolutely mandatory for mathematical physics research, and has been demonstrated in this appendix. The routine used was fairly straight forward to implement. Calculations were done in c++ to allow for fast analysis. Figures A.1 and A.2 display the routine maintaining great stability until the strong dark energy term becomes entirely dominant as  $\eta$  goes to  $\eta_\infty$ . Therefore values extremely close to the asymptote might not be as reliable as others. Though a smaller step size or an improved routine could most likely bury much of the error.

# Appendix B

## Calculation of Elliptic Functions and Integrals

### B.1 Maple

We are blessed to live in an age of almost infinite computational power. Only the most complex problems in physics can not be solved with our technology today. The results obtained in this thesis were calculated using Maple. Maple has functions to directly calculate the elliptic functions of Jacobi and Weierstrass, as well as elliptic integrals.

# Bibliography

- [1] M. Abramowitz and I. Stegun, *Handbook of mathematical functions.*, Dover Publications, New York, 1965.
- [2] P. F. Byrd and M. D. Friedman, *Handbook of elliptic integrals for engineers and scientists*, Springer-Verlag, address = Berlin Heidelberg New York, 1971.
- [3] S. G. Carroll, *Spacetime and geometry: An introduction to general relativity*, Addison Wesley, San Francisco, 2003.
- [4] S. Chandrasekhar, *The mathematical theory of black holes*, Oxford University Press, New York, 1998.
- [5] Planck Collaboration, *Planck 2018 results i. overview and the cosmological legacy of planck*, *Astron. Astrophys.* (2019), 1–56.
- [6] M. Dabrowski and J. Stelmach, *A redshift-magnitude formula for the universe with cosmological constant and radiation pressure.*, *Astronomical Journal* **92** (1986), 1272–1277.
- [7] H. T. Davis, *Introduction to nonlinear differential and integral equations*, Dover Publications, New York, 1962.
- [8] J. D’Ambrose, *Applications of elliptic and theta functions to friedmann-robertson-lemaitre-walker cosmology with cosmological constant*, arXiv:0908.2481v1 (2009), 1–23.

- [9] J. D'Ambroise and F. L. Williams, *Parametric solution of certain nonlinear differential equations in cosmology*, Journal of Nonlinear Mathematical Physics **18** (2011), no. 2, 269–278.
- [10] D. Edwards, *Exact solutions for friedmann models with radiation and the superluminal expansion of the universe*, Astrophysics and Space Science **24** (1973), no. 2, 563–575.
- [11] A. Beléndez et al, *Exact solution for the nonlinear pendulum*, Brazilian Journal of Physics Education **29** (2007), no. 4, 645–648.
- [12] G. F. R. Ellis et al, *Relativistic cosmology*, Cambridge University Press, Cambridge, 2012.
- [13] J. Liske et al, *Cosmic dynamics in the era of extremely large telescopes*, arXiv:0802.1532v1 (2008), 1–27.
- [14] M. V. Sazhin et al, *The scale factor in the universe with dark energy*, arXiv:1109.2258 (2011), 1–20.
- [15] J. P. Mimoso F. S. N. Lobo and M Visser, *Cosmographic analysis of redshift drift*, arXiv:2001.11964v2 (2020), 1–20.
- [16] V. Faraoni, *Natural phenomena described by the same equation*, Eur. J. Phys. (2020), 1–19.
- [17] E. H. Gudmundsson and G. Björnsson, *Dark energy and the observable universe*, Astrophys. J. (2001), 1–16.
- [18] J. B. Hartle, *Gravity: An introduction to einstein's general relativity*, Addison Wesley, San Francisco, 2003.
- [19] D. W. Hogg, *Distance measures in cosmology*, arXiv:astro-ph/9905116 (1999), 1–16.

- [20] L. I. Kharbediya, *Some exact solutions of the friedmann equations with the cosmological term*, Astron. Zh. (1976), 1145–1152.
- [21] G. Lemaître, *Cosmological application of relativity*, Rev. Mod. Phys. (1949), 357–366.
- [22] ———, *The expanding universe*, Gen. Relativ. Gravit. (1997), 641–680.
- [23] C. H. Lineweaver and T. M. Davis, *Expanding confusion: common misconceptions of cosmological horizons and the superluminal expansion of the universe*, arXiv:astro-ph/0310808v2 (2003), 1–26.
- [24] NASA, *Wilkinson microwave anisotropy probe*, <https://map.gsfc.nasa.gov>, 2017, Accessed: 2022-03-17.
- [25] O. F. Piattella, *Lecture notes in cosmology*, arxiv.org:1803.00070 (2018), 13–43.
- [26] A. G. Reiss, *Observational evidence from supernovae for an accelerating universe and a cosmological constant*, Astron. J. (1998), 1009–1038.
- [27] C. M. Rodríguez, *Orbits in general relativity: the jacobian elliptic functions*, Italian Physics Society **98** (1987), 87–96.
- [28] B. Ryden, *Introduction to cosmology*, Cambridge University Press, Cambridge, 2017.
- [29] G. Scharf, *Schwarzschild geodesics in terms of elliptic functions and the related red shift*, J. Mod. Phys. **2** (2011), 274–283.
- [30] W. A. Schwalm, *Lectures on selected topics in mathematical physics: Elliptic functions and elliptic integrals*, Morgan & Claypool Publishers, California, 2015.
- [31] F. Steiner, *Solution of the friedmann equation determining the time evolution, acceleration and the age of the universe*, Conference: Evolution Equations - The State of the Art (Castle Reisenburg, Günzburg, Germany), 2007, pp. 1–17.

- [32] F. Steiner and R. Aurich, *The cosmic microwave background for a nearly flat compact hyperbolic universe*, arXiv:astro-ph/0007264 (2018), 1–8.
- [33] E. T. Whittaker, *A course of modern analysis*, Cambridge University Press, Cambridge, 1927.
- [34] Wikipedia, *Jacobi elliptic functions*, [https://en.wikipedia.org/wiki/Jacobi\\_elliptic\\_functions](https://en.wikipedia.org/wiki/Jacobi_elliptic_functions), 2023, Accessed: 2023-03-26.